LEVEL III

U.S. Department of Transportation

Federal Aviation Administration

Office of Environment
and Energy
Washington, D.C. 20591

AD A097607

Nitric Oxide Measurement Study:

Comparison of Optical and Probe Methods. Volume III.

A097545

DTIC
SELECTED
APR 1 0 1981

C

DTIC FILE COPY

1. Report No.	2. Government Accession No.	3. Recipient's Catalog No.
FAA-EE-80-30	AD-D091 667	

4. Title and Subtitle	5. Report Date
Nitric Oxide Measurement Study: Comparison of Optical and Probe Methods • Volume III	March 31, 1980
	6. Performing Organization Code

7. Author's) M. F. Zabielski, L. G. Dodge, M. B. Colket, III, D. J. Seery	8. Performing Organization Report No. R80-994150-3

9. Performing Organization Name and Address	10. Work Unit No. (TRAIS)
United Technologies Research Center Silver Lane E. Hartford, CT 06108	
	11. Contract or Grant No. DOT FA77WA-4081
	13. Type of Report and Period Covered

12. Sponsoring Agency Name and Address	
U.S. Department of Transportation Federal Aviation Administration Office of Environment and Energy Washington, DC 20591	
	14. Sponsoring Agency Code

15. Supplementary Notes Funding for this study was provided by an Interagency Committee. Contributing agencies and report nos. are: DOT-FAA (FAA-EE-80-30); USAF (ESL-TR-80-15); NASA (CR-159863); USN (NAPC-PE-39C); EPA (EPA-460/3-80-015).

16. Abstract

Nitric oxide (NO) was measured in the exhaust of three different combustion systems by in situ ultraviolet absorption and by chemiluminescent analysis after gas sampling with several probe designs. The three combustion systems were: (1) a flat flame burner fueled with $CH_4/N_2/O_2$; (2) a research swirl burner fueled with C_3H_8/air; and, (3) a modified FT12 combustor operated on Jet A/air. Each combustion system was run at several different conditions so that probe and optical measurements could be obtained over a wide range of exhaust environments encompassing products from lean, stoichiometric, and rich flames, laminar to turbulent flows, and temperatures at centerline from 600 K to 1800 K. The results obtained with the metallic, water-cooled probes of different designs (all expansion-type) agreed with the optical results to within 25 percent. Some small losses of NO (10-15 percent) were observed in a lean methane flame at 1800 K with an uncooled stainless steel probe, but under fuel-rich conditions up to 80 percent NO destruction was observed. Experimental facilities are described, previous results are discussed, and a summary of the major findings of this study is given.

The Nitric Oxide Measurement Study is in three volumes:
Optical Calibration — Volume I;
Probe Methods — Volume II;
Comparison of Optical and Probe Methods — Volume III.

17. Key Words	18. Distribution Statement
Nitric oxide, ultraviolet absorption, probe sampling, chemiluminescent analysis, combustion.	Document is available to public through the National Technical Information Service, Springfield, VA 22161

19. Security Classif. (of this report)	20. Security Classif. (of this page)	21. No. of Pages	22. Price
Unclassified	Unclassified	95	

Form DOT F 1700.7 (8-72) Reproduction of completed page authorized

ACKNOWLEDGMENTS

ABSTRACT

Nitric oxide (NO) was measured in the exhaust of three different combustion systems by in situ ultraviolet absorption and by chemiluminescent analysis after gas sampling with several probe designs. The three combustion systems were: (1) a flat flame burner fueled with $CH_4/N_2/O_2$; (2) a research swirl burner fueled with C_3H_8/air; and, (3) a modified FT12 combustor operated on Jet A/air. Each combustion system was run at several different conditions so that probe and optical measurements could be obtained over a wide range of exhaust environments encompassing products from lean, stoichiometric, and rich flames, laminar to turbulent flows, and temperatures at centerline from 600 K to 1800 K. The results obtained with the metallic, water-cooled probes of different designs (all expansion-type) agreed with the optical results to within 25 percent. Some small losses of NO (10-15 percent) were observed in a lean methane flame at 1800 K with an uncooled stainless steel probe, but under fuel-rich conditions up to 80 percent NO destruction was observed. Experimental facilities are described, previous results are discussed, and a summary of the major findings of this study is given.

R80-994150-3

Nitric Oxide Measurement Study:
Comparison of Optical and Probe Methods

TABLE OF CONTENTS

TABLE OF CONTENTS (Cont'd)

LIST OF FIGURES

LIST OF TABLES

LIST OF TABLES

I. INTRODUCTION

Since Johnston (1971) and Crutzen (1970, 1972) independently suggested that the injection of nitric oxide (NO) into the upper atmosphere could significantly diminish the ozone (O_3) concentration, an accurate knowledge of the amount of NO emitted by jet aircraft has been a serious concern to those involved in environmental studies. This concern intensified when McGregor, Seiber, and Few (1972) reported that NO concentration measured by ultraviolet resonant spectroscopy were factors of 1.5 to 5.0 larger than those measured by extractive probe sampling with subsequent chemiluminescent analysis. These initial measurements were made on a YJ93-GE-3 engine as part of the Climatic Impact Assessment Program (CIAP) which was one of four studies (CIAP, NAS, COMASA, COVOS (see References)) commissioned to determine the possible environmental consequences of high altitude aircraft operation, especially supersonic aircraft. After those studies were initiated, economic factors strongly favored the production and operation of subsonic aircraft. Nevertheless, since the subsonic aircraft fleet is large and does operate as high as the lower stratosphere, interest in the causes of the discrepancies between the two NO measurement methods continued. Few, Bryson, McGregor, and Davis (1975, 1976, 1977) reported a second set of measurements on an experimental jet combustor (AVCO-Lycoming) where the spectroscopically determined NO concentrations were factors of 3.5 to 6.0 higher than those determined by the probe method. In this set of measurements, optical data were obtained not only across the exhaust plume but also in the sample line connecting the probe with the chemiluminescent analyzer. The sample line optical data seemed to agree with the chemiluminescent analyzer data, hence, it was suggested that the discrepancies were due to phenomena occurring in the probe. These results stimulated a third set of measurements involving ultraviolet spectroscopy (Few et al, 1976a, 1976b), infrared gas correlation spectroscopy (D. Gryvnak, 1976a, 1976b) and probe sampling on an Allison T-56 combustor. The measured ratios of the ultraviolet to the probe values typically ranged between 1.5 and 1.9 depending on the data reduction procedure. The ratios of the infrared to the probe values varied between 1.1 to 1.5 also depending on the method of data reduction. In addition to these engine and combustor data, evidence supportive of the accuracy of the ultraviolet spectroscopic method, i.e., calibration data and model predictions, was presented by McGregor, Few, and Litton (1973); Davis, Few, McGregor and Glassman (1976); and Davis, McGregor, and Few (1976). Nevertheless, it was still not possible to make a judgment on the relative accuracy of the spectroscopic and probe methods. The most significant reasons for this were: the complexity of the spectroscopic theory and computer model required to infer concentration from optical transmission; the inadequate treatment of probe use; and the incomplete exhaust temperature and pressure data which are necessary for a valid comparison of the methods. Recently, Oliver et al (1977, 1978) as part of the High Altitude Pollution Program has ranked these discrepancies as a major and a continuing source of uncertainty in atmospheric model predictions.

The purpose of this investigation was to identify and determine the magnitude of the systematic errors associated with both the optical and probe sampling techniques for measuring NO. To accomplish this, the study was divided into three parts. The first was devoted to calibrating the ultraviolet and infrared spectroscopic methods. This entailed developing procedures which could provide known concentrations of NO over a wide range of temperatures and pressures, and also reviewing and correcting the ultraviolet spectroscopic theory used in the engine and combustor measurements cited above. The results of this part are presented in TASK I Report entitled Nitric Oxide Measurement Study: Optical Calibration by Dodge et al (1979). The second part of this study was focused on sample extraction, transfer, and analysis of chemiluminescent instrumentation. The sampling methods were used on three successively more complicated combustion systems starting with a flat flame burner and culminating with a jet combustor. The results are presented in TASK II Report entitled Nitric Oxide Measurement Study: Probe Methods by Colket et al (1979). In the third part of this study, optical measurements were made on the same three combustion systems operated at the same conditions used for the probe measurements. The results of the optical and probe measurements were compared and are given in this the TASK III Report entitled Nitric Oxide Measurement Study: Comparison of Optical and Probe Methods.

The main elements of this report, i.e., TASK III, are the following. First, the flat flame burner, swirl combustor, and jet combustor are described, and typical NO concentration and temperature distributions are given. The probes, both sampling and temperature, used to obtain these distributions are also described. Second, the details of both ultraviolet and infrared spectroscopic systems are provided. The procedures for interpreting the optical data are reviewed. Third, the results of the optical measurements are compared with the probe sampling results for all three combustors. Fourth, a review is presented of previous work in which optical and probe sampling measurements of NO were compared. Finally, a summary of the major conclusions of this study are given.

II. APPARATUS

II.A General

As part of the method to identify the relative merits of probe and optical measurements of NO in the exhaust of aircraft engines, three combustion systems of varying degrees of complexity were used. These systems were:

1. $CH_4/O_2/N_2$ flame over a flat flame burner:
    $\phi = 0.8$, 1.0, 1.2, P = 1 atm, $\dot{m}_{TOTAL} \sim 2.75$ g/sec

2. C_3H_8/Air flame in a swirl burner:
    $\phi = 0.8$, 1.0, 1.2, Swirl = 0.63, and 1.25, P = 1 atm, $\dot{m}_{TOTAL} \sim 71$g/sec

3. Jet A/Air flame in a modified FT12 combustor: Idle, Cruise, and Maximum Continuous, P = 1 atm, $\dot{m}_{TOTAL} \sim 470$g/sec.

Physical details and operation of the flat flame burner are described in TASK I Report (Dodge, et al., 1979); consequently, only a brief overview will be presented here. For the other two flames, each burner assembly could be installed separately into a single combustor housing with the associated fuel lines and flow controls modified accordingly. This facility and the burner assemblies are described in detail in this chapter. In addition, techniques for temperature measurements with corrections for radiation and conduction, sample gas transfer and analysis, are presented.

II.B Flat Flame Burner

The flat flame burner is made of sintered copper and has two zones: the main zone (containing the main flame seeded with nitric oxide) with dimensions of 17.5 x 9.2 cm or 161 cm^2 and the (unseeded) buffer zone with an area of 76 cm^2. A methane flame was burned above the buffer flame to provide a hot zone in the wings of the flame. The burner was enclosed by a stainless steel shroud/chimney with optical ports to separate windows (quartz or salt) from the flame. The ports were purged with nitrogen at room temperature to reduce the local nitric oxide concentrations within these ports. A top view of the burner is shown in Figure II-1. Temperatures were measured using a butt-welded, Ir/60% Ir-40% Rh thermocouple coated with a mixture of Yttrium and Berylium oxides. The diameter of the bead and coating was approximately 90 microns (0.0035 inches). Gases were individually metered using critical flow orifices. Separate mixes of gases (N_2, O_2, CH_4, NO, H_2, Ar) were blended for the main and buffer flows. Details of these facilities are provided in the Task I Report (Dodge, et al, 1979). The flames examined in this program are listed in Table II-A.

TOP VIEW OF FLAT FLAME BURNER AND ASSEMBLY

FIG. II-1

QUARTZ WINDOWS

DEAD SPACE

S S SHROUD

BUFFER ZONE

INERT
GAS PURGE

MAIN GAS FLOW
(SEEDED W/NO)

SCALE

5 cm
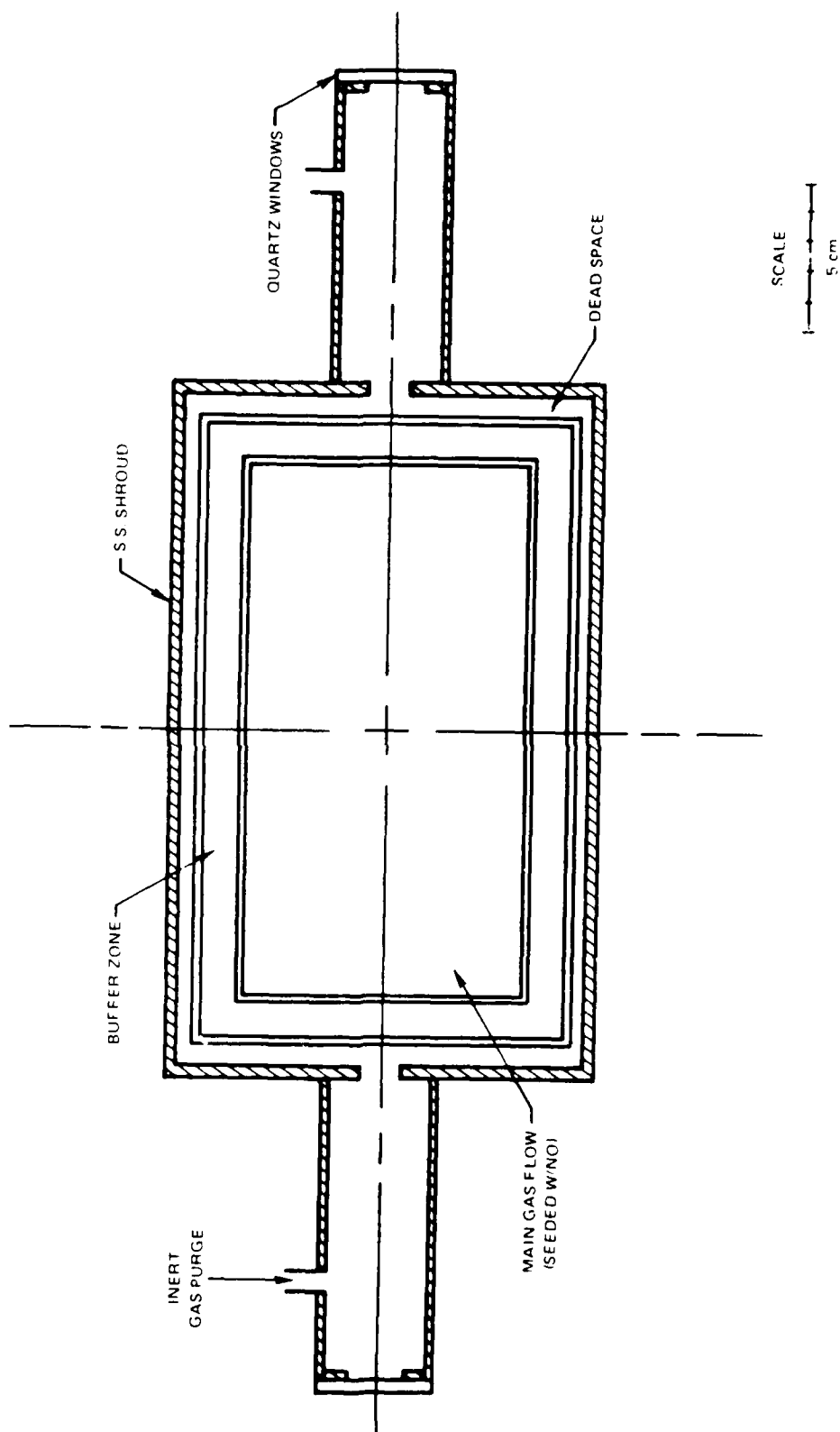
TABLE II-A

OPERATING CONDITIONS FOR THE FLAT FLAME BURNER[*]

Test Condition	B1	B2	B3
$\dot{m}_{N_2}$ (g/sec)	2.15	2.20	2.07
$\dot{m}_{O_2}$ (g/sec)	0.512	0.466	0.494
$\dot{m}_{CH_4}$ (g/sec)	0.103	0.116	0.149
T_{inlet} (K)	285	285	285
P (psia)	14.7	14.7	14.7
ϕ	0.8	1.0	1.2

---

[*]Without Seed

II.C Large Scale Combustor Test Section

The combustor test section used for the swirl burner and FT12 combustor is shown schematically in Fig. II-2. It consists of a water-cooled, double-walled chamber 50 cm in diameter (i.d.) and 150 cm long. Four (4) rows of eight (8) viewing ports are provided in the combustor section at 90° intervals. It was constructed at UTRC specifically to investigate flame phenomena with various optical and probing techniques. The two burner systems were designed to fit inside the burner housing. One is a swirl burner and is a scaled down version of the burners designed at the International Flame Research Foundation (IFRF). The second is a modified FT12 burner and shroud. The optical axis used for subsequent optical measurements was the center of the third window from the far right in Fig. II-2. All probes (sample and thermocouple) were designed to translate across this axis.

II.C.1 IFRF burner

The IFRF burner assembly, as shown in Fig. II-3, is a model of those burners described by Beér and Chigier (1972) and consists of a central fuel nozzle and an annular air supply. A movable vane block arrangement provides variable air swirl intensity from a swirl number of 0 to 2.5; in this case, the swirl number is defined as the ratio of the tangential to the axial momentum divided by the radius of the exit quarl. The swirl number was calculated using the appropriate equations in the text by Beer and Chigier (1972) and, as they demonstrate, experimental and theoretical values agree fairly well for this type of burner. An axially adjustable, 19 mm diameter, fuel feed tube can be equipped with various pressure atomizing or air-assisted fuel spray nozzles.

This swirl burner has been tested previously during internal programs at UTRC and has been used recently to study the combustion of a coal/oil slurry (Vranos, et al, 1979). In this study, gaseous propane was used for fuel and a nozzle was constructed to inject the fuel radially into the swirling air flow. Six stable operating conditions were selected for these tests and provide three stoichiometries and two swirls. Input conditions are listed in Table II-B. The optical axis and the probe tips were located 87.5 cm downstream of the quarl exit.

The two swirl levels used in these tests (0.63 and 1.25) were selected by performing a series of tests on flame stability. At lower swirl numbers, the propane flame was relatively long and unstable and was not considered to be suitable for this series of tests. Beér and Chigier argued that below a swirl number of 0.6 axial pressure gradients are insufficient to cause internal recirculation; however, at higher swirl intensities a recirculating zone in the central portion of the jet is required to support a strong adverse pressure gradient along the axis. Since recirculation zones tend to stabilize the flame and increase the intensity of reaction, the ability to achieve stable flame conditions only above swirl numbers of 0.6 in this research program is in agreement with Beér and Chigier's analysis.

FIG II-2

ATMOSPHERIC PRESSURE COMBUSTION FACILITY

TRANSITION DUCT

WATER-COOLED, DOUBLE-WALLED, CONSTRUCTION

4 ROWS OF 8 QUARTZ WINDOWS

COMBUSTOR SECTION (60 IN. LONG X 20 IN. DIA)

SWIRL BURNER

FUEL

AIR

79-06-11-5

FIG 11-3

SWIRL BURNER ASSEMBLY

STATIC PRESSURE

FUEL

COOLING WATER

SWIRL VANE ADJUSTMENT/INDICATOR

STATIONARY VANES

MOVEABLE VANES

AIR

SWIRL VANES

SWIRL VANE ARRANGMENT

FUEL NOZZLE

AERODYNAMIC PROBE

NECK

QUARL
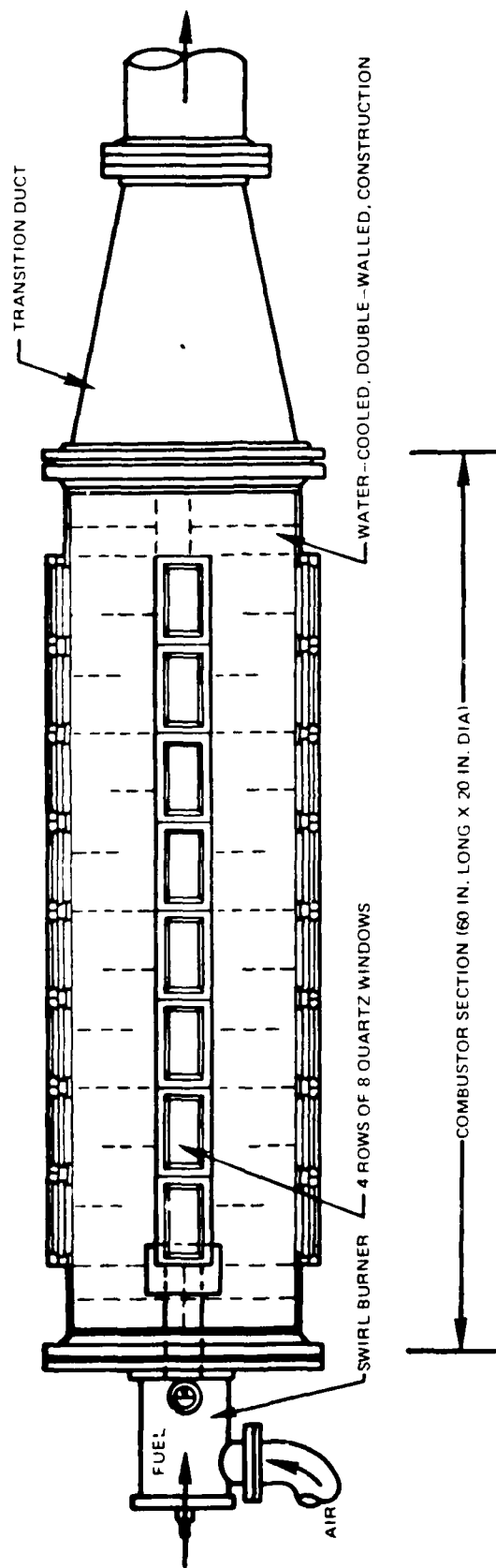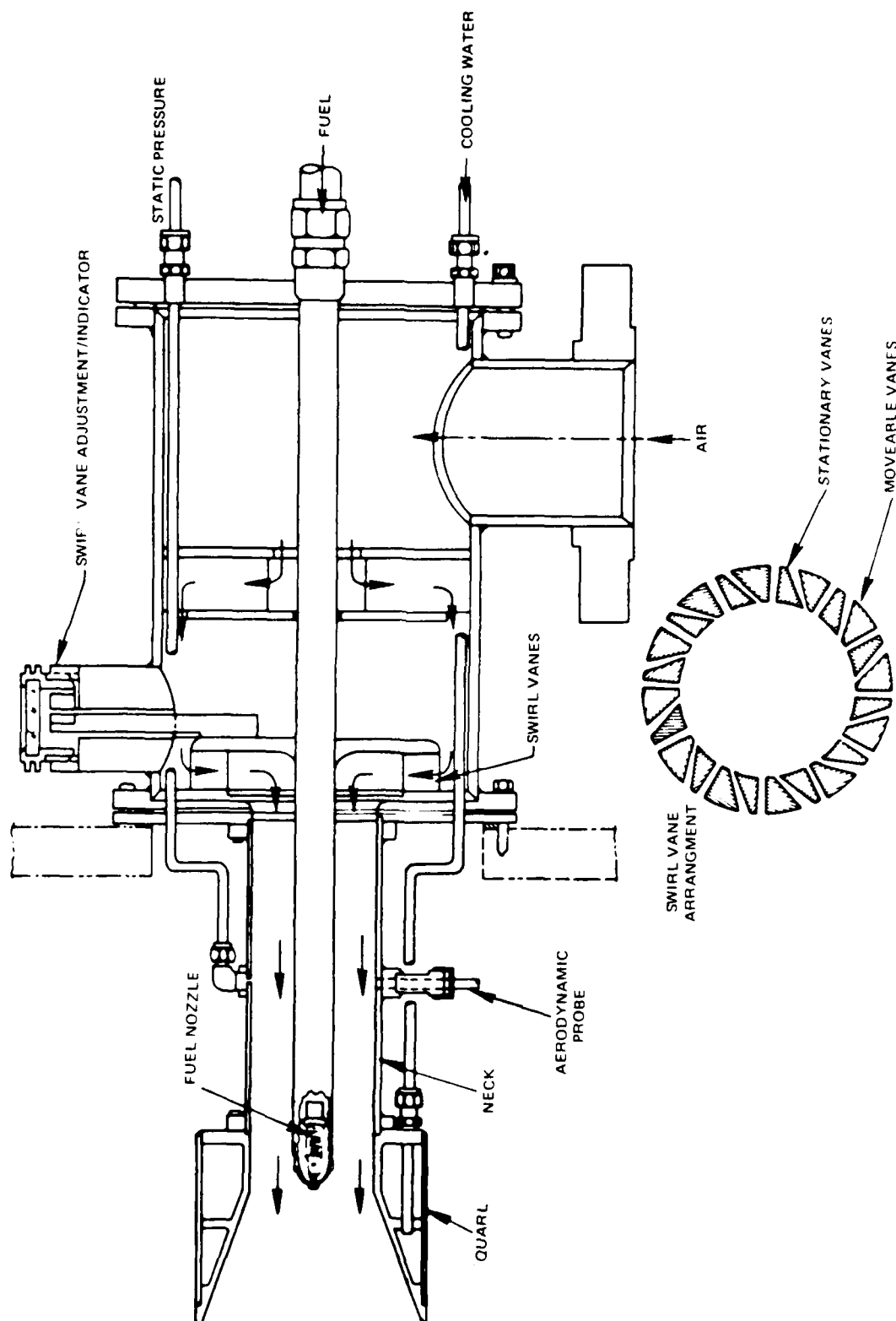
TABLE II-B

OPERATING CONDITIONS FOR THE IFRF BURNER

Test Condition	1, 4[+]	2, 5[+]	3, 6[+]
m_{air} (g/sec)	66.7	66.7	66.7
P (psia)	14.7	14.7	14.7
T_{inlet} (K)	290	290	290
$\dot{m}^{*}_{fuel}$ (g/sec)	3.40	4.26	5.11
ϕ	0.8	1.0	1.2

---

* Gaseous propane

+ Swirl number (see definition in text) was 0.63 for test conditions 1-3 and 1.25 for test conditions 4-6.

II.C.2 FT12 Burner Can

A modified FT12 combustor can used in this program was 29.5 cm in length (11.5 cm shorter than the original can) and 13.0 cm in diameter. It was altered to make all air addition holes symmetric. This can was welded at its exit to a shroud and was placed in the test section with the swirl burner removed. As shown in Fig. II-4, a flow straightener was placed in the burner housing upstream of the combustor can and appropriate fuel lines and cable for spark ignition were fed through the housing. A standard fuel nozzle for the FT12 (Pratt & Whitney Part No. 525959) was used in this series of tests.

Three flight conditions, i.e. idle, cruise, and maximum continuous, were simulated. A simulation was necessary since the test section could only sustain a maximum pressure of four atmospheres, while the cruise and maximum continuous flight conditions required pressure above six atmospheres.

In addition, since gas sampling and accurate definition and examination of the optical path is simplified by operating at one atmosphere, all experiments were performed at one atmosphere. Simulated flight conditions at this lower operating pressure, were calculated by equating Mach numbers. This is a common test procedure and is useful in simulating equivalent fluid flow patterns and heat transfer. In this case, the mass flow rate was reduced appropriately to maintain the chamber pressure at one atmosphere and the inlet temperature was identical to the flight conditions. The simulated flight conditions are listed in Table II-C. The optical and probe axis was 78 cm downstream from the exit of the FT12 burner can.

II.C.3 Temperature Measurements

Exhaust temperatures from the IFRF and FT12 combustors were made using a water-cooled, double shielded, aspirated thermocouple probe with a bead made of Pt/Pt-13%Rh. The probe was manufactured by Aero Research Instrument Co. (Part Number T-1006-6 (25) R) according to specifications described by Glawe, et al. (1956) but was modified (by water cooling and material substitution) to increase the temperature range to above 1370 K (2000°F). A photograph of this probe is shown in Fig. II-5. Radiation and conduction corrections were made according to equations supplied by the manufacturer. For the measurements made in this study (P = 1 atm, Mach No. << 1), these equations can be written

$$T_{gas} (K) = T_{thermocouple} (K) + \Delta T_{RC}$$

where the radiation and conduction correction, ΔT_{RC}, is given by

$$\Delta T_{RC} = \frac{0.55 \; C_1}{\sqrt{M}} (K)$$

$$C_1 (K) = 0.00917 \; T_{thermocouple} (K) - 7.136$$

FIG II-4

FT12 ASSEMBLY

FUEL

IGNITER CABLE

FLOW STRAIGHTENER

~ 1/3 ACTUAL SIZE

AIR

MODIFIED FT12 BURNER CAN
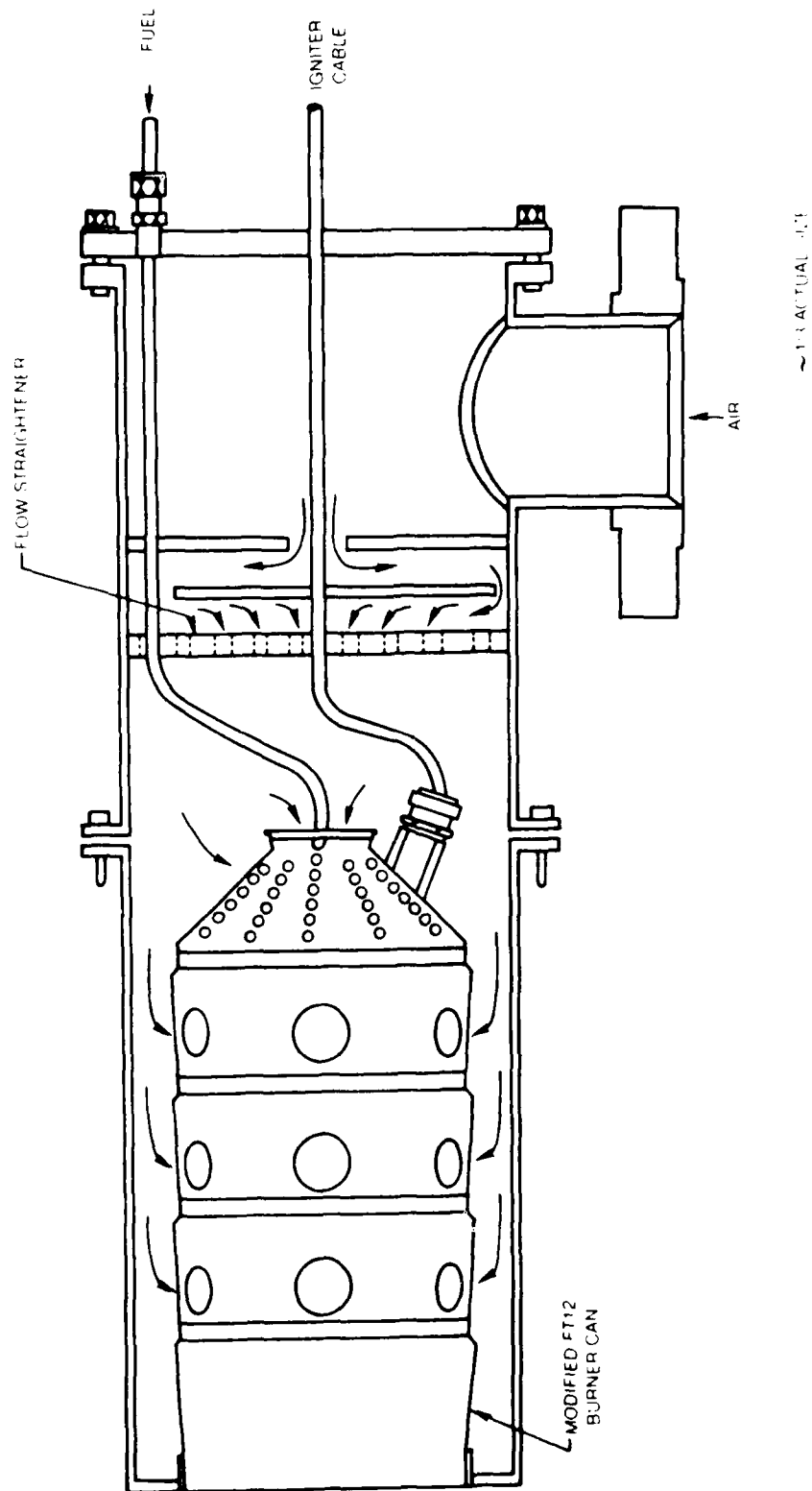
79-10-85 16

TABLE II-C

OPERATING CONDITIONS FOR THE FT12 COMBUSTOR

	Idle	Cruise	Maximum Continuous
$\dot{m}_{air}$ (g/sec)	485	463	454
P (psia)	14.7	14.7	14.7
T_{inlet} (K)	335	515	524
$\dot{m}^*_{fuel}$ (g/sec)	5.15	6.62	6.92
f/a	.0106	.0143	.0152

---

*Jet A

FIG II-5

Pt-Pt/13% Rh ASPIRATED THERMOCOUPLE
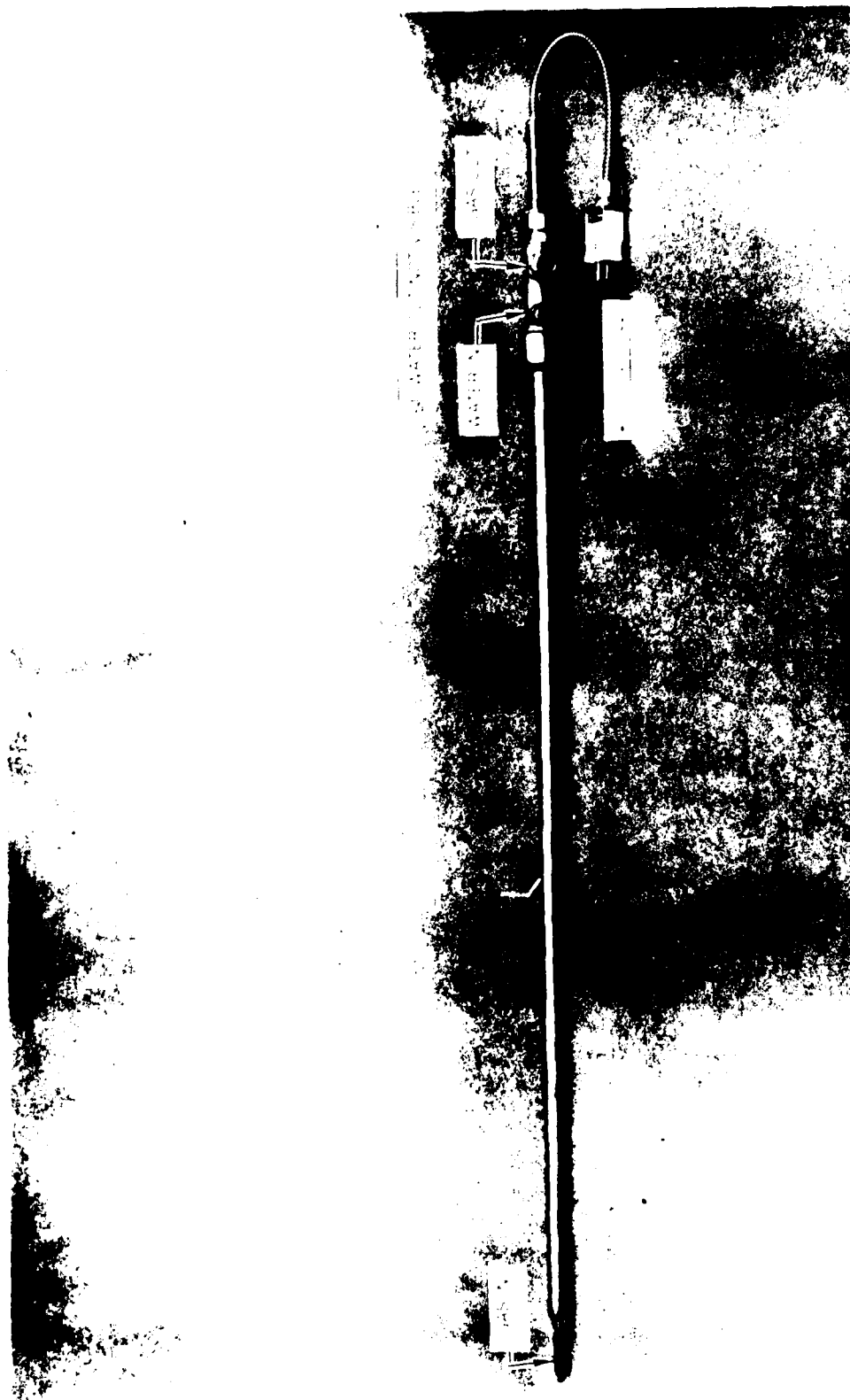
and M is the Mach number. For the FT12, no correction was made since ΔT_{RC} was negligible (< 10 K). For the IFRF burner, corrections were typically on the order of 50 K. Additional description on the operation of aspirated probes is given by Land and Barber (1954).

II.D Sampling Systems

Two instrumentation systems were used for measuring the products of combustion. The first is the Scott Exhaust Analyzer used in the Task I of this program and the second is a chemiluminescence analyzer made by Thermo Electron Corporation (TECO). The Scott system was used during the initial tests with the flat flame burner to obtain concentrations of the major species. The Scott system was thereafter dedicated to the larger scale combustor tests and the TECO instrument was used for subsequent measurements of NO/NO_x over the flat flame burner. The Scott system was dedicated to the combustor measurements for two reasons. First of all, it was impractical to move this system between facilities and secondly it was determined that the Scott package (under the conditions of the flat flame tests) did not satisfy the Federal requirements for total instrument response time and could not be easily modified to meet those requirements.

II.D.1 Scott Exhaust Analyzer

The Scott Model 119 Exhaust Analyzer provides for the simultaneous analysis of CO, CO_2, NO or NO_2, O_2 and total hydrocarbons (THC). The analyzer is an integrated system, with flow controls for sample, zero and calibration gases conveniently located on the control panel. The incoming gas sample passes through a refrigeration condenser ($\sim 275K$), to remove residual water vapor. As the sample passes from the condenser, it is filtered to remove particulate matter. The system is comprised of five different analytical instruments. Beckman Model 315B Non-Dispersive Infrared (NDIR) Analyzers are used to measure the CO and CO_2 concentrations in the gas sample. Concentration ranges available on the CO analyzer were from 0-200 ppm to 0-15% on several scales. Concentration ranges available on the CO_2 analyzer were 0-4% and 0-16%. The accuracy of the NDIR analyzers is nominally $\pm$ 1% of full scale. A Scott Model 125 Chemiluminescence Analyzer is used to measure the NO and NO_2 concentrations in the gas sample. Concentration ranges available with this instrument were from 0-1 ppm to 0-10,000 ppm on several scales, with a nominal $\pm$ 1% of full scale accuracy. The thermal converter used in the chemiluminescent analyzer was stainless steel, and was operated at a temperature of approximately 1000 K. A Scott Model 150 Paramagnetic Analyzer is used to measure the O_2 concentration in the gas sample. Concentration ranges available with this instrument were from 0-1% to 0-25% on several scales, with a nominal accuracy of $\pm$ 1% of full scale. A Scott Model 116 Total Hydrocarbon

Analyzer is used to measure the hydrocarbon concentration in the gas sample. This analyzer utilizes an unheated flame ionization detection system to provide for measurement of hydrocarbons (as methane) in concentration ranges from 0-1 ppm to 0-10%, with a nominal accuracy of $\pm$ 1% of full scale. Output signals from the various analyzers are displayed on chart recorders and a digital display.

The sample line was teflon-lined aluminum. The typical operating temperature was 380 K. When sampling from the large combustors, water was removed from the sample by two traps cooled to 3° C. The first was located 6 ft. beyond the probe exit and the second was housed in the Scott analyzer.

II.D.1a Pumping Requirements

Two problems specific to this sampling/probe system were encountered. First of all, the orifice diameter of the macroprobes (2mm) was sufficiently large that a separate vacuum pump (17.5 cfm) was required to reduce the back pressure of the probe to the very low values ($\sim$ 1/10th of an atmosphere) required in this program. This vacuum pump was attached directly to the probe via a line one inch (2.54 cm) in internal diameter and three feet (90 cm) long. The second requirement was that, at the reduced pressures, the pumping capacity of the sampling system must be sufficient to deliver flow to the analytical instrumentation. To accomplish this task, a MB-301 pump and two MB-118 pumps (metal bellows) were assembled in a series/parallel arrangement. These pumps were in addition to the two MB-118 pumps in the Scott analyzer and the vacuum pump associated with the CLA. Even with this pumping capacity the deliverable flow was marginal at the lowest of probe back pressures.

II.D.2 TECO Analyzer

The Thermo Electron Corporation (TECO) Model 10AR Chemiluminescent NO/NO$_x$ analyzer was used for the reported data for the flat flame burner. This instrument has a stated minimum detectable concentration of 50 ppb and a maximum limit of 10,000 ppm. Linearity within any of its eight operating ranges is given as $\pm$ 1%. A TECO Model 300 Molybedenum NO$_x$ Converter was used for the NO$_2$ determinations. Sample was delivered to this analyzer at atmospheric pressure by a metal bellows pumps (Metal Bellows MB-118). The sample line was 12 ft of treated teflon line (Technical Heaters, Inc.). The back pressure of the probe was continuously monitored using a Matheson test gauge (0-760 torr, absolute).

II.E Probes

As outlined in TASK II Report (Colket et al, 1979), a probe must be designed for the combustion system being investigated. As a result, the probes

used for the flat flame burner measurements were significantly different from those used for the large scale combustor measurements. The two most important criteria for designing probes can be summarized by the following. First, the presence of the probe should introduce a minimal perturbation to the temperature of the sampled media. In the post flame or exhaust gases, larger perturbations can be tolerated than in the flame front gases. Second, the quenching of the reactions in the sampled gases by static temperature and pressure reduction must be rapid. The minimum quenching required is determined from kinetic considerations.

II.E.1 Flat Flame Burner

The four probes used for the flat flame burner measurements were all expansion-type and classified in TASK II Report (Colket et al, 1979) as mini-probes. The major distinctions between a miniprobe and the classical microprobe (Fristrom and Westberg, 1965) are the orifice dimension and the area ratio, i.e., the miniprobe has a larger orifice and a smaller area ratio than those of the microprobe. In either type, however, the principal mechanism for quenching was convective cooling and not aerodynamic cooling. Four types of miniprobes were used, each of which had an orifice dimension of 0.025 inches (635 microns). The first of these was entirely stainless steel with a water-cooling channel. A schematic and photograph are shown in Figures II-6 and II-7, respectively. The second water-cooled probe was identical to the first with the exception that its tip was copper. The purpose for the copper tip was to decrease the time spent by the sampled gases in contact with high temperature walls. The third probe was water-cooled quartz similar to that used in TASK I (Dodge et al, 1979); however, its orifice was enlarged to the above dimension. The fourth probe was uncooled stainless-steel. The tip and internal geometry were identical to the metallic water-cooled probes; however, the external diameter was 0.635 cm versus 0.95 cm because the cooling passages were not present.

II.E.2 Large Scale Combustors

Two water-cooled probes were designed to make measurements on the IFRF and FT12 combustors. These probes have been defined as the reference probe and the EPA probe. The geometries of these probes are depicted in Fig. II-8. The important distinction between these probes is that the reference probe is cap-able of being operated in the aerodynamic quench mode. The EPA probe can achieve quenching only via the convective process. It has been defined as the EPA probe, because it conforms to the present requirements for a probe which are given in the Federal Register (1972, 1976). The reference probe can also be operated in the convective quenching mode. When operated in this mode, it also satisfies the Federal Register requirements. Figure II-9 shows the tip of the reference probe. Figure II-10 shows the complete reference probe assembly.

FIG 11-6

DRAWING OF MINIPROBE

0.95cm

0.254cm

H_2O in

H_2O out

TIP

2.74cm

890μm

635μm
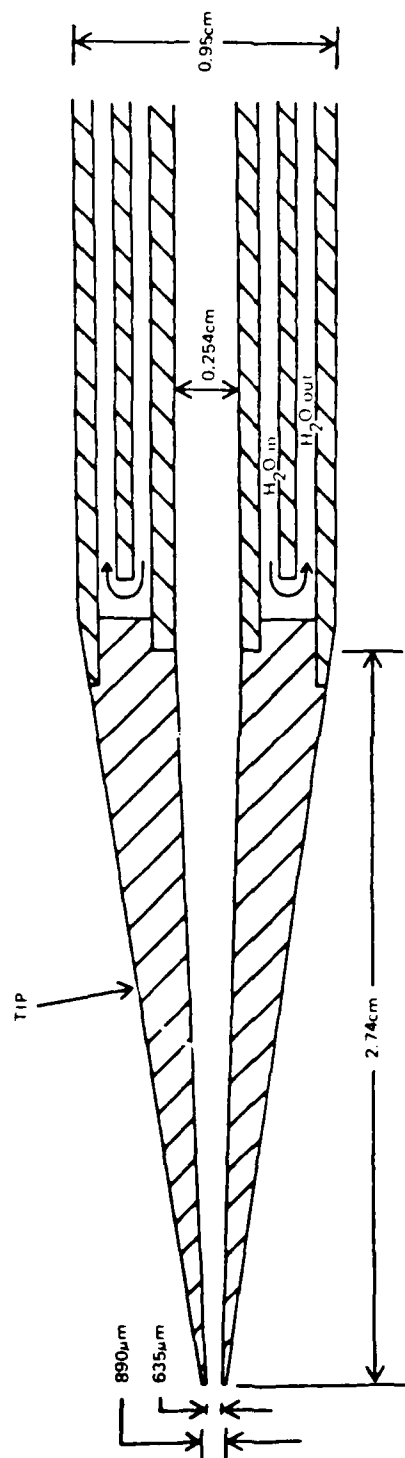
FIG II-7

STAINLESS STEEL TIPPED MINIPROBE

ORIFICE 6 µm MICRONS

GAS SAMPLE OUT

WATER IN AND OUT

FIG II-8

DRAWINGS OF MACROPROBES

REFERENCE PROBE

EPA PROBE

H_2O out

H_2O in

H_2O out

H_2O in

1.09cm

1.9cm

0.65cm

24.6cm

21cm

10.2cm

2.5cm

3.3cm

0.20cm

1.9cm

6.35cm

0.31cm

24.6cm

10.2cm

0.95cm

0.5cm

0.20cm

79-10-85-23
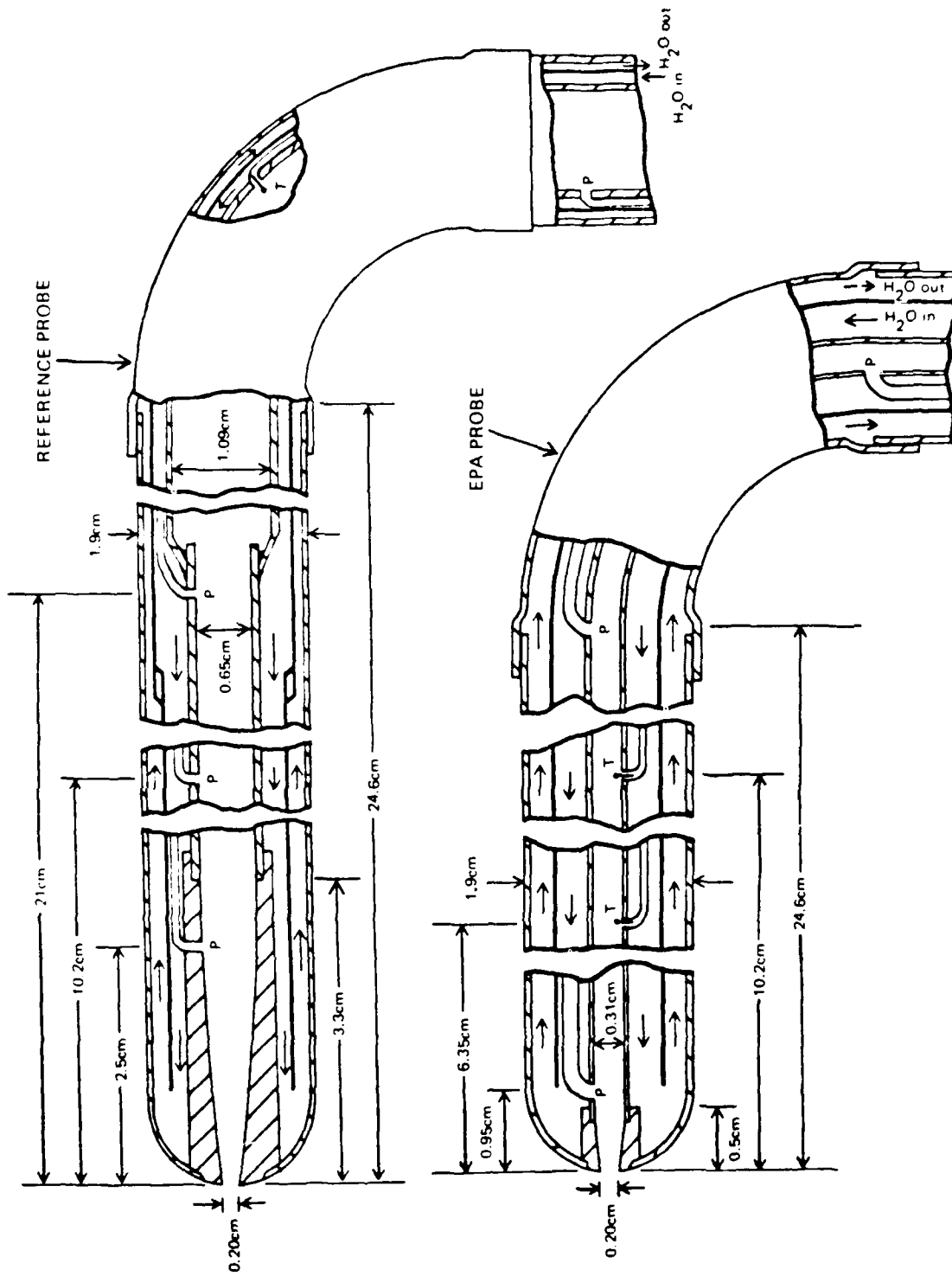
FIG II-9

TIP OF REFERENCE PROBE

FIG II-10

REFERENCE PROBE

GAS SAMPLE

PRESSURE TAPS (4)

DIA THERMOCOUPLE WIRES (2)

WATER COOLING FOR PROBE

WATER-COOLED MOUNT

0 5 10
CENTIMETERS
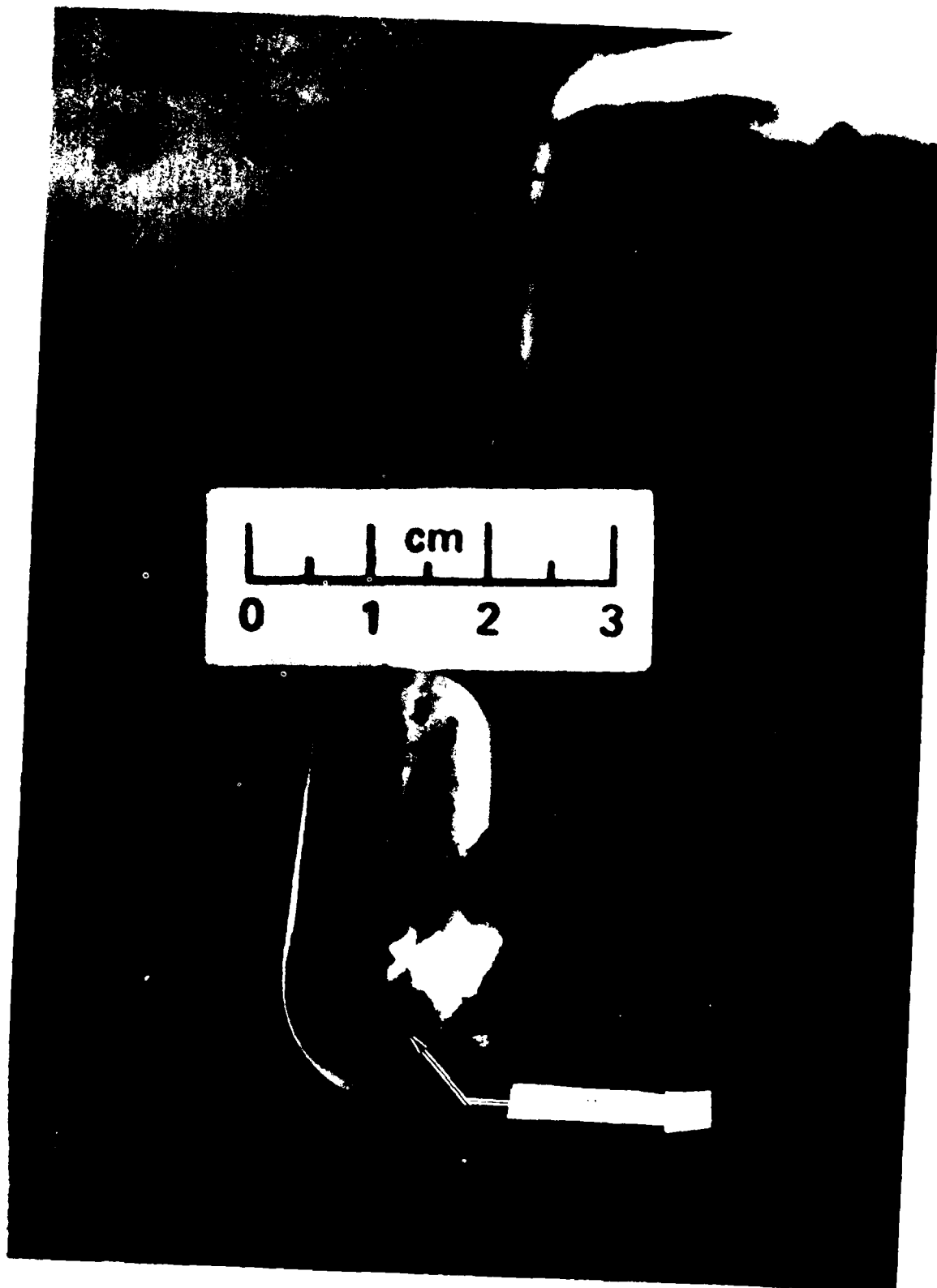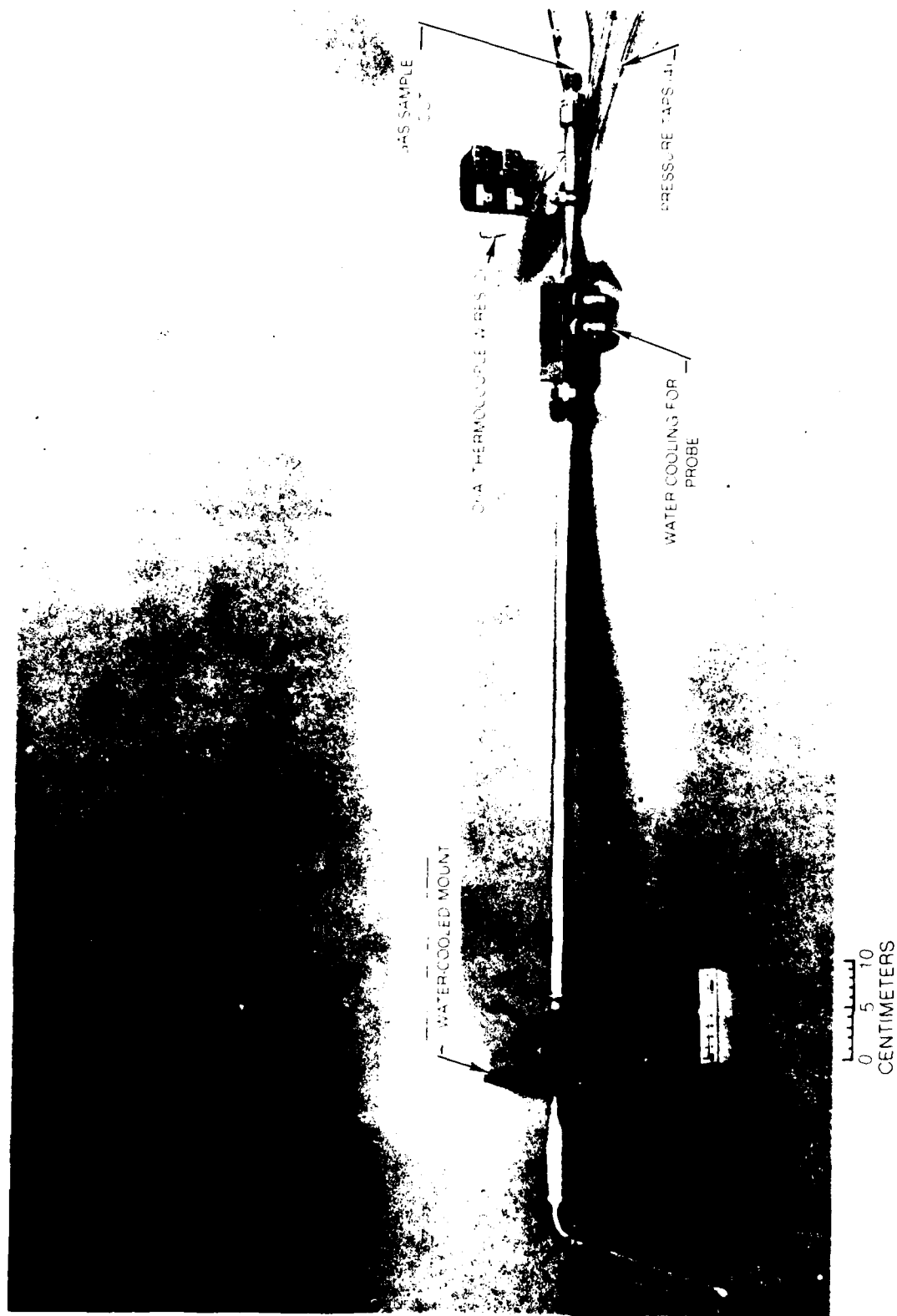
II.F Optical Apparatus

The ultraviolet optical instrumentation used for the in situ NO
determinations was chosen based on ambient conditions. Since the flat flame
burner was operated in a laboratory where vibrations were minimal and temper-
ature was held at a near constant value, high resolution measurements were
possible. However, vibrations and large ambient temperature excursions in
large scale combustor facilities permitted only low resolution measurements
on the IFRF and FT12 combustors.

II.F.1 Flat Flame Burner

The apparatus used for the flat flame burner measurements was similar to
that employed in TASK I Report (Dodge et al, 1979). Two distinct light sources
were used. The first was a hollow cathode lamp which produced emission lines
mainly from NO, N_2 molecules and ions, and Ar. The spectral lines of interest
were the NO $\gamma(0,0)$, $\gamma(1,1)$, $\gamma(2,2)$, and $\gamma(3,4)$. For reference, a succinct dis-
cussion of the spectroscopy of NO is included in TASK I Report (Dodge et al,
1979). This lamp is shown in Fig. II-11. Its design was based on that of Meinel
(1975). Typical discharge conditions were 25 ma at 2 torr in flowing air. It
should be noted that there are some spectral lines due to species other than NO
in the $\gamma(0,0)$ region. The effect of these lines is discussed in TASK I Report
(Dodge et al, 1979). The second lamp used was a 1000 W high pressure Xe arc
lamp (Conrad-Hanovia 976C-0010) mounted in an Oriel housing. The center of the
optical beam was located 2.0 cm above the top of the burner.

A 1.5-m focal length J-Y spectrometer in a temperature controlled box with
a 2400 g/mm holographic grating (110 x 110 mm), aperture of f/12, and Fastie
curved slits was employed for all flat flame measurements. Typical slit
function, full width at half maximum (FWHM), was observed to be 0.0018 nm with
7 μm slit settings for the 226 nm NO lines observed in the 2nd order of the
grating. Most of the spectra were recorded with a Hamamatsu R166 solar blined
(Cs-Te photocathode) photomultiplier tube cooled to -30 °C in a Products for
Research TE-177 thermoelectrically cooled housing.

The signal from the photomultiplier was amplified with an Analog Devices
AD310K used in the electrometer mode with feedback components of R_f = 100 M and
C_f = 5000 pf. The scan rate was 3.95 x 10^{-4} nm/sec. The resulting spectra
were recorded with a Hewlett-Packard 7100B strip chart recorder. In the case
of the continuum lamp, some of the spectra were corrected for lamp drift by a
ratiometric technique. This involved a reference measurement of the source
lamp prior to any absorption, and was accomplished by placing a flat mirror
slightly off the edge of beam directed through the calibration apparatus which
reflected light through a 226 nm filter and onto an EMI 9601B photomultiplier

WATER COOLED HOLLOW CATHODE LAMP

tube. The signal from the spectrometer was divided by this reference signal in an Ithaco model 3512 ratiometer and this resultant ratio was recorded on the strip chart recorder. This ratiometric technique reduced but did not eliminate baseline drift in the recorded spectra while using the continuum lamp.

The ultraviolet radiation from the source lamp was collimated and directed through the 12.7 mm diameter apertures, across the flat flame burner, and then imaged on the spectrometer slit using fused silica lenses.

The spectrometer was operated in high resolution and low resolution. The slits were set at about 5 to 10 μm for the high resolution work, corresponding to slit functions with FWHM of about 0.0015 nm to 0.0025 nm. The slits were set at 1380 μm for the low resolution studies, with a FWHM value of 0.146 nm.

II.F.2 Large Scale Combustors

For the measurements on the IFRF and FT12 combustors, only the hollow cathode lamp was employed. The radiation from this lamp was collimated into a 38 mm diameter beam by a quartz lens. The optical path through the expansion chamber was a nominal 70 cm. Since windowless ports were used on the expansion chamber, the actual optical path containing significant quantities of NO was dependent on operating conditions. The beam was then focused into a 0.5 m Czerny-Turner spectrometer manufactured by SPEX. The spectrometer was equipped with a 1200 g/mm grating which was used in second order. The slit function was 0.146 nm full width at half height. A solar blind detector (Hamamatsu R166) was cooled to -30 C. The grating control circuitry was modified to perform precise repetitive scans over a selected region. This modification allowed signal averaging to improve the signal-to-noise ratio. The output of the detection electronics, which were operated in a dc mode, was recorded and summed in a Northern Scientific NS575 signal averager with a NS580 module. The contents of the NS575 memory were then recorded on 7 track digital tape by a NS408F/Wang Mod 7 tape system.

III RESULTS

III.A. General

In order to reduce the optical data and to compare optical and probe results, complete profiles of temperature and NO concentration are required. For brevity, only selected profiles obtained on the various combustors will be presented here. Additional detailed profiles are given in Appendix A which contains the results of the infrared measurements. The temperature profiles in the appendix are the same as those which existed when the ultraviolet measurements were made; however, the centerline concentrations of NO were considerably higher than those of the ultraviolet measurements. The normalized profiles are, on the other hand, quite similar.

The optical data were reduced using a first principles computer model which is described in TASK I Report (Dodge et al, 1979). To compare NO measurements determined optically with those determined by probe/chemiluminescent analysis, it is important to recognize that the optical method determines the number of molecules per unit volume for an optical path under isothermal and isobaric conditions. The probe method, on the other hand, determines its result in mole fraction (ppmv) irrespective of the temperature and pressure at the probe orifice. If the temperature and pressure are known along the optical path, it is straightforward to effect a comparison. In combustion systems, however, gradients in temperature and pressure are encountered; thus more effort is required to perform the comparison. The approach developed by Gryvnak and Burch (1976a, b) for their infrared measurements and subsequently adopted by Few et al (1976) for their ultraviolet measurements is the correct approach. With this approach, the optical path is divided into isothermal regions. The mean value of the NO number density is computed from the probe determined mole fraction, temperature, and static pressure for each of the isothermal zones. This information is then used to compute the optical transmission for each region. The total transmission is determined by multiplying the zonal transmissions together. (In this study, six or more zones were employed.) This procedure is based on a Beer's Law relationship between number density and optical thickness and, thus, it is assumed that "line-center burnout" (see TASK I Report I, Dodge et al, 1979) is not present. For all the results, which will be presented below, this procedure was used and the absence of "line-center burnout" is an excellent assumption. The probe calculated transmission will be called τ_c. This calculated transmission will be compared with the optically measured transmission τ_m.

In order to determine τ_m, it was necessary to account for intensity changes due to beam-steering, scattering by particulates, continuum-type absorption by other molecules and drifts in lamp intensity and electronics. This was accomplished by monitoring "reference" bands emitted by the hollow-cathode

lamp. Specifically, these bands were the NO $\gamma(3,4)$ and $\gamma(2,2)$ bands. No appreciable absorption by NO occurs in these bands because these states are not significantly populated at temperatures up to 2000K.

Finally, the quantitative comparison between the probe and optical measurements is defined for the hollow cathode (narrow-line) lamp as

$$\frac{[NO]_p}{[NO]_{nl}} = \frac{\ln\tau_c}{\ln\tau_m^{nl}} \qquad (III-1)$$

and for the continuum lamp

$$\frac{[NO]_p}{[NO]_{cl}} = \frac{\ln\tau_c}{\ln\tau_m^{cl}} \qquad (III-2)$$

where [NO] represents the NO concentration, and subscripts (superscripts) p, nl, and cl represent probe, narrow-line, and continuum lamp. Ratios greater than 1 indicate that the probe determined NO concentrations are greater than the optically determined NO concentrations. Ratios less than 1 indicate that the optically determined NO concentrations are greater than the probe determined NO concentrations.

III.B. Flat Flame Burner

Two separate types of ultraviolet measurements were made on the flat flame burner. The first was made with the hollow cathode (narrow-line) lamp; the second was made with the continuum lamp. The results of both these measurements are compared with the probe measurements.

III.B.1. Probe Measurements

As outlined in Section II.E, four probes were employed in making measurements. For the three water-cooled probes, the NO concentrations determined were the same within the experimental precision ($\sim$10%). In order to insure unambiguous optical measurements, i.e., absorptions greater than 10 percent, the flames were seeded with NO.

Three flame stoichiometries, $\phi = 0.8$, 1.0, and 1.2, were examined and the specifics of these run conditions are listed in Table II-A. With the nitrogen

purge passing through the optical ports, vertical and horizontal temperature profiles were obtained. A typical horizontal profile (for $\phi = 0.8$) is shown in Fig. III-1. These measurements are corrected for radiation losses as outlined in Task I Report by Dodge, et al. (1979) and were obtained along the optical axis. The burner surface was located 2 centimeters below this axis while the visible flame sheet was a few millimeters above the burner surface; hence, these were exhaust stream measurements. Estimates of uncertainties in the radiation corrections and individual and repeated measurements are indicated in the error bars. Vertical profiles of uncorrected thermocouple temperatures for the three flames are shown in Fig. III-2. Since the optical beam is less than a centimeter in diameter and centered at 2 centimeters above the burner, the beam encompasses a region for which deviations (due to height) are less than $\pm$ 15K. As may be observed by comparing these two figures, radiation corrections at the centerline are on the order of 140 K for these flames.

Measurements of stable species using the Scott Instrument package and the quartz, water-cooled probe (all water-cooled probes produced the same results within 10 percent) are reproduced in Table III-A. Equilibrium data at the adiabatic flame temperature (Gordon and McBride, 1971) for the flat flames are also presented in this table for comparison. It may be noted that reasonable agreement is obtained between the measured and equilibrium values. Noticeable differences are observed for the CO and CO_2 concentrations. Although these differences may be due to interconversion within the probe, it is also possible to attribute these to differences in actual and adiabatic flame temperatures and to incomplete combustion of carbon monoxide. Only in the case of the stoichiometric case ($\phi = 1.0$) is the measured total of the CO and CO_2 concentration significantly different from the equilibrium calculations ($\sim 8\%$). (Data on unburned hydrocarbons are not reported since their concentration even in the fuel-rich flame were less than 1000 ppm.)

Measured concentrations of nitric oxide were on the order of 5, 30, and 30 ppm for the three flames, respectively. These values at flame temperatures and for the given optical path length are much smaller than that necessary to produce a reasonable signal-to-noise ratio for the optical measurements described here. For the path length and temperatures encountered, concentrations of 700-1500 ppm were required for the unambiguous UV resonant lamp measurements and even higher NO densities were required for the infrared gas correlation technique. Consequently, all subsequent studies were made using nitric oxide premixed with the inlet gases.

Using the stainless steel tipped, water-cooled probe and the TECO CLA, nitric oxide horizontal profiles were obtained for a given seed level. Profiles, normalized to the input seed level for the flames $\phi = 0.8$ and $\phi = 1.2$ are shown in Fig. III-3. Data for the $\phi = 1.0$ flame is nearly identical to the data for the $\phi = 0.8$ flame except the centerline fraction is slightly higher (~ 0.88) for an NO seed level of 840 and 980 ppm calculated on a wet and dry basis, respectively. For the lean flame, NO_x values were typically 5 to 7 percent higher than the NO and, for the stoichiometric and rich flames, they were about

FIG III-1

HORIZONTAL TEMPERATURE PROFILE OVER CH₄/O₂/N₂ FLAT FLAME

ϕ 0 R

O THERMOCOUPLE TEMPERATURE
   CORRECTED FOR RADIATION

TEMPERATURE (K)

POSITION FROM CENTERLINE (CM)

79-10-85-13

FIG III-2

VERTICAL TEMPERATURE PROFILE OVER $CH_4/O_2/N_2$ FLAT FLAME

○ ϕ = 0 8
△ ϕ = 1 0
□ ϕ = 1 2

UNCORRECTED FOR RADIATION

TEMPERATURE (K)

HEIGHT ABOVE BURNER (CM)

79-10-85-14

III-5
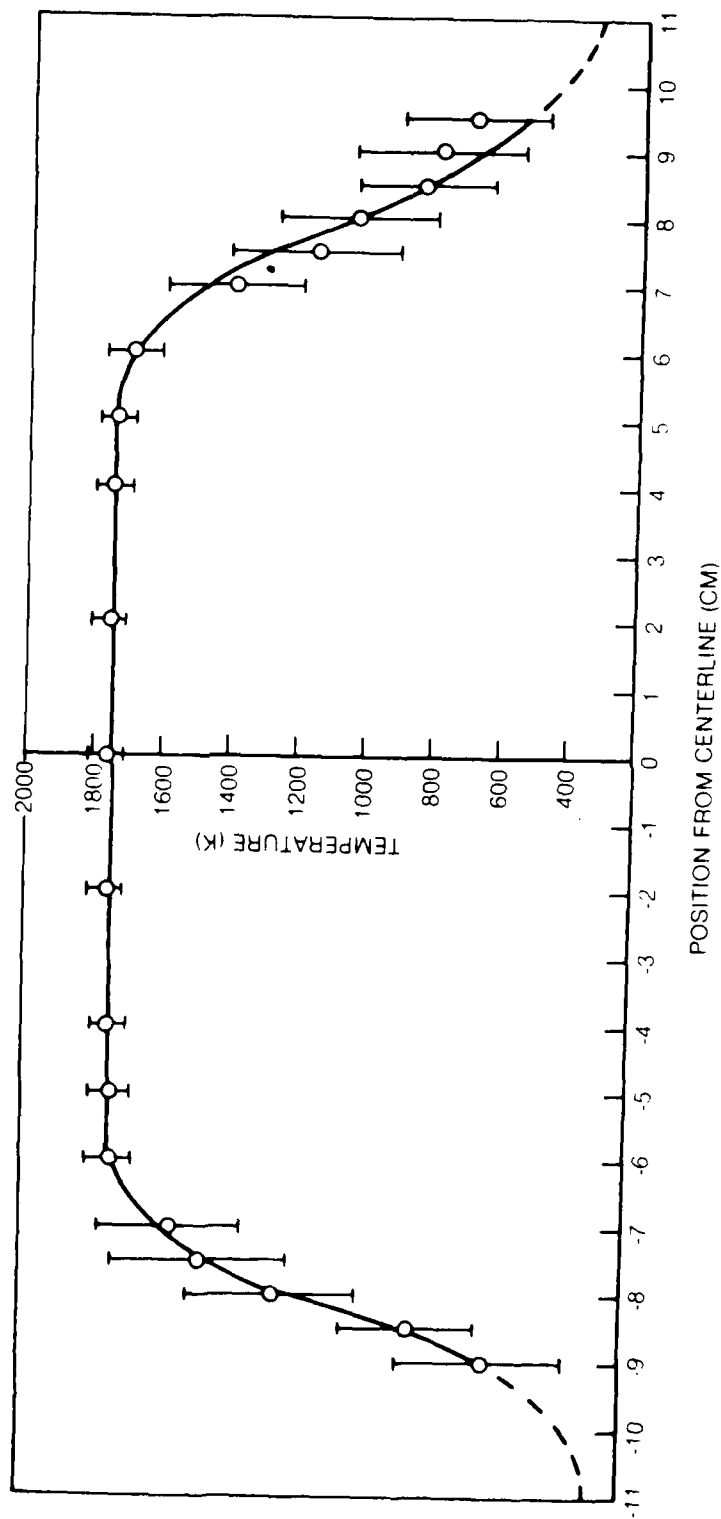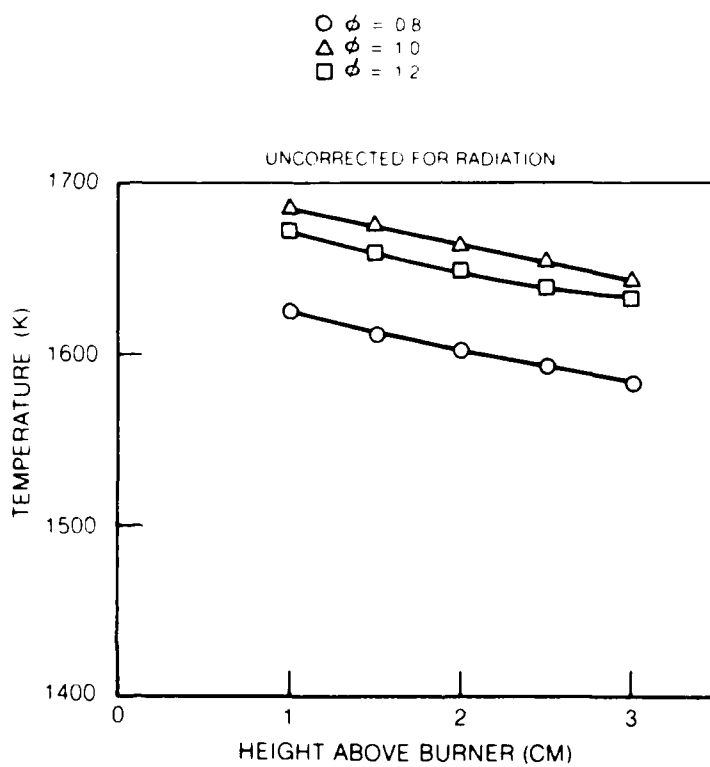
TABLE III-A

MOLE PERCENT OF STABLE SPECIES FOR
THE FLAT FLAME BURNER
(Wet Basis)

Experimental

ϕ	O_2[1]	CO[1]	CO_2[1]	H_2O[2]	N_2[3]	Temp. (K)
0.8	3.2	.0137[4]	6.6	12.6	77.6	1740
1.0	0.2[4]	.064	6.55	14.1	78.7	1815
1.2	–	4.1	4.8	17.8	73.3	1800

Equilibrium[5]

ϕ	O_2	CO	CO_2	H_2O	N_2	Temp. (K)
0.8	3.15	0.0051	6.43	12.9	77.4	1765
1.0	0.13	0.109	7.09	14.3	78.1	1905
1.2	0.7ppm	3.60	5.50	15.7	72.6	1904

1. Measured values but corrected for the presence of water vapor.
2. Water estimated from known input conditions.
3. Nitrogen calculated by difference.
4. Error $\pm$ 40% of value.
5. Based on equilibrium flame temperature.

Except where noted, the uncertainty of the experimental concentrations is approximately $\pm$ 5% of reported (experimental) value.

NORMALIZED NITRIC OXIDE PROFILES OVER $CH_4/O_2/N_2/NO$ FLAT FLAME

FIG III-3

79-10-85-12
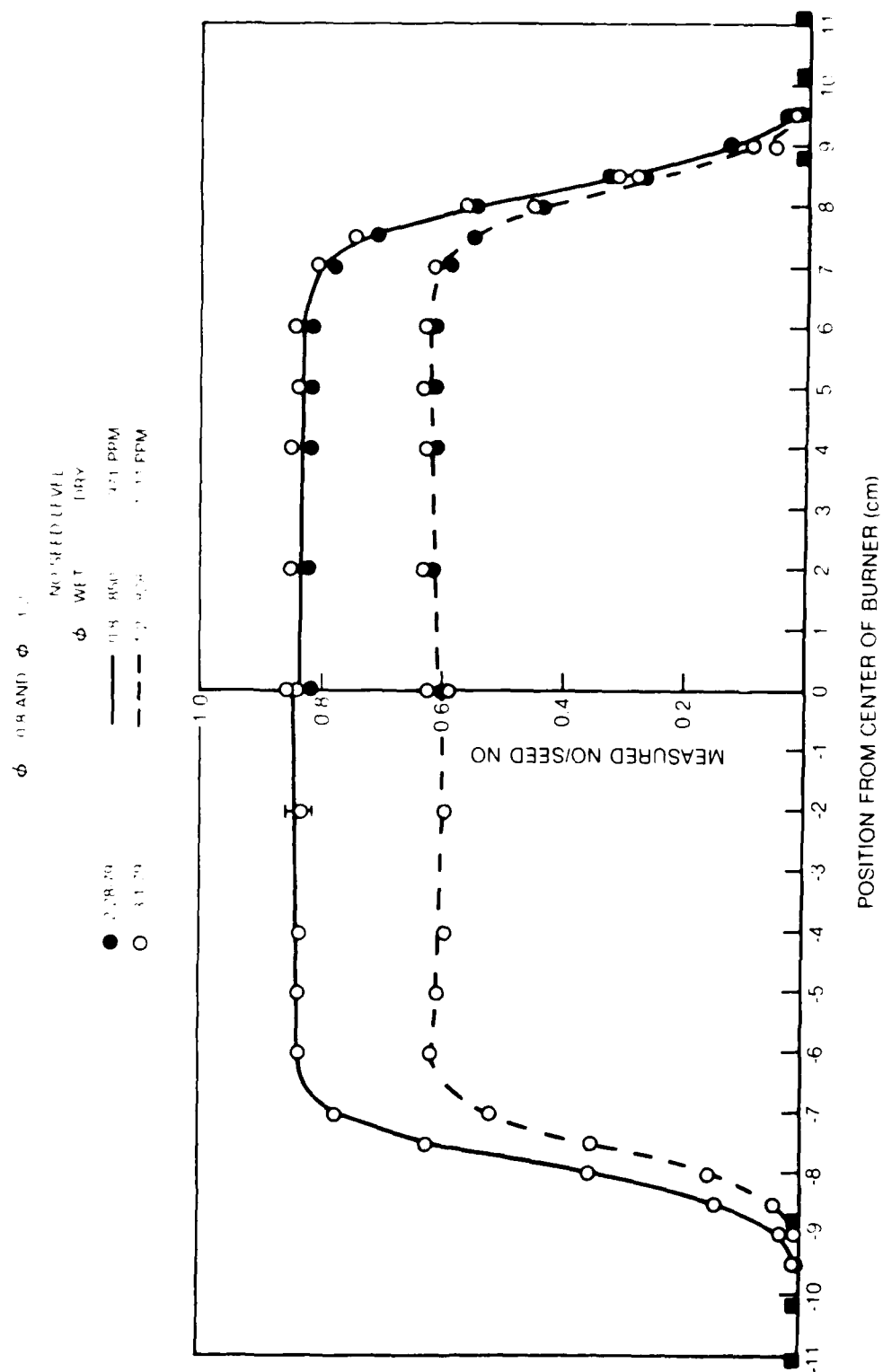
3 percent higher than measured NO. The excellent repeatability of the burner and sampling conditions is indicated by the double set of points on the right-hand side of this figure.

Vertical profiles for the three flames and the three water-cooled probes are reproduced in Fig. III-4. Agreement between these profiles is generally quite good (within 6%) except for relatively low values obtained by the stainless steel tipped probe when sampling the rich flame. Since the front part of this tip ($\sim$ 1 cm) becomes very hot (with a red-orange glow), it is believed that catalytic reactions take place similar to that occurring in an NO_2 to NO converter. This conclusion is consistent with the computed results from TCAL (see TASK II, Colket et al, 1979) indicating that the stainless steel tip is insufficiently cooled. Although residence times in this portion of the probe are very short ($\ll$ 1 msec), the wall temperatures very near the orifice are significantly hotter than in a stainless steel converter (1100 to 1200 K vs. 1000 K). The profile may be associated with the presence of hydrogen that would be expected to decrease with height above the flame. Although this mechanism was not verified, it seems highly likely considering the strong NO_x reducing effect that hydrogen has in hot stainless steel tubes (Benson and Samuelsen, 1976, 1977). The relatively low values obtained in the $\phi = 0.8$ flame for the copper-tipped probe are unexplained. Although this difference of 7 percent may be due to a catalytic effect of a copper surface, it is unclear why good agreement is found for the other flames. In any case, this difference is considered to be small.

From the above results, it is seen that the recovery of the nitric oxide needed into the flame is not complete. At the seed concentrations, approximately 15, 12, and 38 percent of the initial NO was lost for the $\phi = 0.8$, 1.0, and 1.2 flames, respectively. Attention was directed at determining whether the loss occurred in the inlet gas lines (for the unburned/premixed gas), in the flame itself, or the probe/sampling system. Losses in the post-flame zone were believed to be unlikely since essentially flat vertical profiles were obtained (Fig. III-4).

These loss figures can be slightly adjusted to account for phenomena associated with the flame and experimental apparatus. First of all, some NO_2 was present as indicated by NO_x readings, and, consequently, the percent losses can be decreased by 3 to 5 percent. Although it is not possible to ascribe the presence of NO_2 to the flame or probe, the fraction of NO_2 was not large enough relative to experimental uncertainties to warrant a detailed investigation. Alternatively, if one assumes that the NO formed in the flame without seed NO is also formed when NO is added, then the losses in the stoichiometric and rich cases can be increased by approximately 3 percent (about 30 ppm in 1000). The estimated losses at centerline of NO may be decreased by about 3 to 5 percent due to dilution from the nitrogen purge in the optical ports (see Dodge, et. al., 1979). Uncertainties also include the inaccuracies

VERTICAL PROFILES OF NITRIC OXIDE OVER FLAT FLAME BURNER

○ S S TIPPED
△ Cu TIPPED   WATER COOLED PROBES
□ QUARTZ

$\phi = 0.8$
SEED 971 PPM

$\phi = 1.0$
SEED 980 PPM

$\phi = 1.2$
SEED 1011 PPM

MEASURED NO CONCENTRATIONS (PPM) (WET)

HEIGHT ABOVE BURNER (CM)
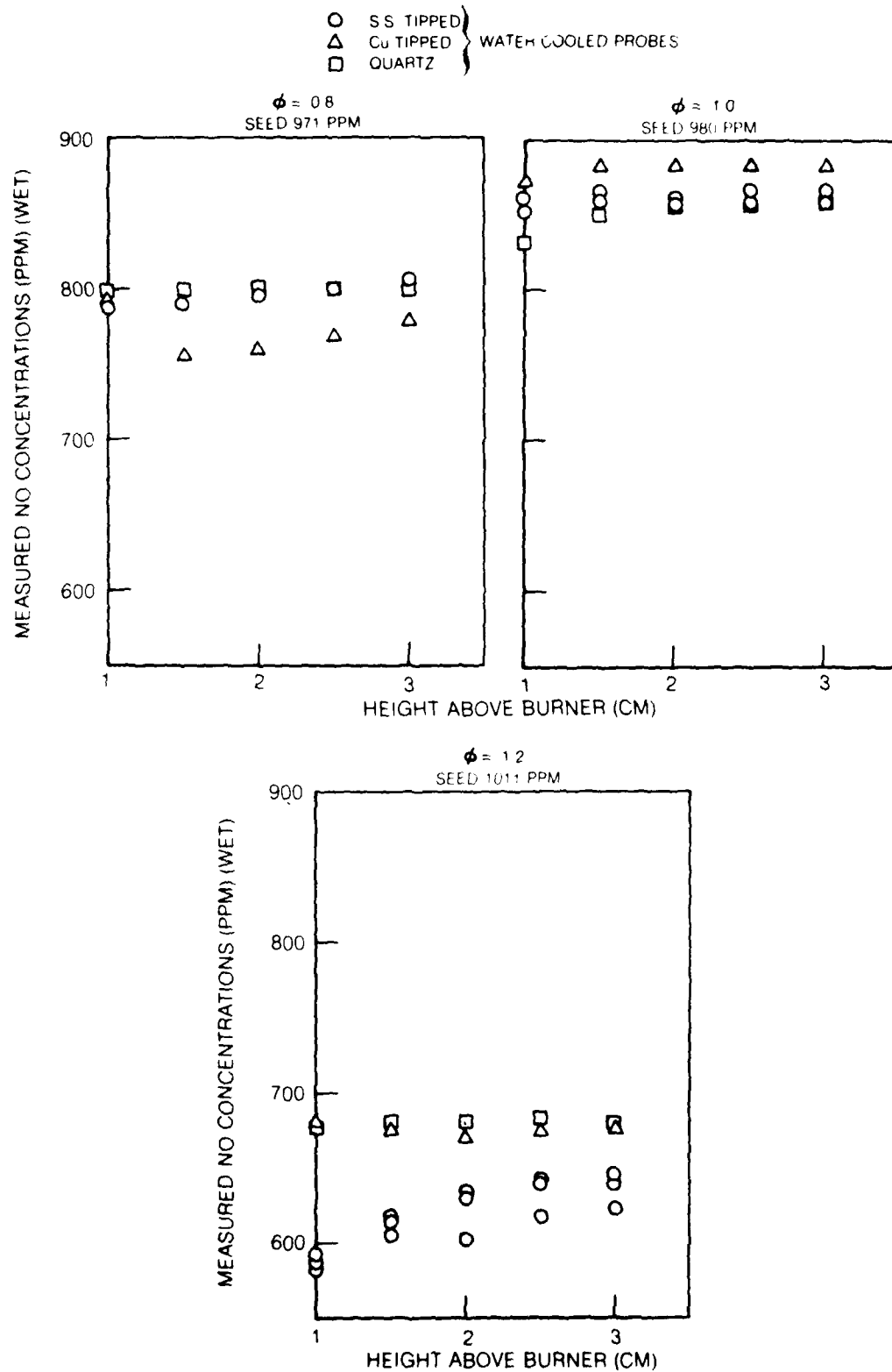
79-10-85-11

in blending from the mixing apparatus and in the calibration and analysis. It is estimated that the sum of these uncertainties is on the order of 3 percent since measured NO concentrations generally agreed to within 3 percent of the calculated values when NO was blended only with nitrogen, and the gas sample was extracted within 1 mm of the burner surface with no flame present and with the nitrogen purge off.

With all of the adjustments and uncertainties mentioned above, the percent NO_x lost for these flames becomes 9, 8 and 34 percent respectively with an uncertainty of about $\pm$ 5 percent in each number, i.e., for the lean flame, the estimated real loss can range from 4 to 14 percent. If the natural NO formed in the flame is not included, then these numbers become 9, 5, and 31 percent for the $\phi = 0.8$, 1.0, and 1.2 flames, respectively.

An uncooled stainless probe geometrically similar to the other metallic probes was also used. This probe, as expected, glowed red when placed in the exhaust of the flame. Using this probe, NO measurements were similar (within 10%) to measurements obtained when using the cooled probes for the lean flames although the results were somewhat dependent on the residence time of the uncooled probe in the flame. Data are reported in Table III-B and times between scans are typically 5-10 minutes. For the stoichiometric flame, the observed NO was approximately 25-30 percent less, and for the rich flame values ranged from the same as that measured using cooled probes to only 20 percent of that value depending on probe history and probe back pressure, i.e., residence time. For example, at 220 torr back pressure and when the flame is quickly changed from the lean to rich flame ($\sim$ 15-30 seconds), cooled and uncooled probes behave similarly but in less than a minute the indicated NO begins to fall and after 10 to 15 minutes a stable, but lower value (by a factor 0.67) is obtained. Then by increasing the back pressure to 430 torr which correspondingly increases the residence time substantially, the NO drops further to only 20 percent of the initial value.

The behavior of the uncooled probe is not unexpected since similar results have been obtained by England, et. al., (1973) and since similar effects are common for a stainless steel NO_2-NO converter when sampling rich flame gases.

III.B.2 Optical Measurements

III.B.2.a Narrow-line Lamp Measurements

For these measurements, the temperature profiles were divided into three zones on each side of the centerline of the burner. Broadening parameters a' for each zone were computed using the broadening coefficients (K) obtained by Dodge et al (1979) and the equilibrium mole fractions for each of the stoichiometries considered. For these atmospheric pressure flames, a' was typically 0.50 in the highest temperature zones ($\sim$ 1830K) and 1.50 in the low temperature zones ($\sim$ 750K). A summary of these measurements is presented in Table III-C.

TABLE III-B

MEASURED CONCENTRATION OF NO (PPM) USING
UNCOOLED, STAINLESS STEEL PROBE OVER FLAT FLAME BURNER[5]

ϕ		0.8^1	0.8^2	1.0^1	1.2^1	1.2^2	1.2^3	1.2^4
height	1.5	772	717	655	242	227	225	147
above	2.0	762	712	630	237	222	217	142
burner	2.5	755	710	545	232	220	215	137
(cm)	3.0	752	702	500	230	215	215	132
Back pressure (torr)		225	213	219	218	218	218	435
Direction of Scan		down	down	down	down	down	up	down
Seed level (ppm)		971	971	980	1011	1011	1011	1011

1. First scan
2. Second scan
3. Third scan
4. Fourth scan
5. These data may be compared directly to data for cooled probes presented in Figure III-4.

TABLE III-C

COMPARISON OF NITRIC OXIDE RESULTS OBTAINED WITH WATER-COOLED
PROBES AND NARROW-LINE ULTRAVIOLET ABSORPTION: METHANE FLAT FLAMES

ϕ	$[NO]_p$ Centerline (wet) (ppmV)	a (Centerline)	1st Bandhead τ_m	1st Bandhead τ_c	2nd Bandhead τ_m	2nd Bandhead τ_c	$\dfrac{[NO]_p}{[NO]_{nl}}$ (AVE.) ($\pm 1\sigma$)
0.8	1997	0.60	0.772 0.787	0.780	0.713 0.727	0.698	1.05±0.07
1.0	1862	0.51	0.821 0.817 0.824	0.794	0.758 0.755 0.760	0.721	1.16±0.03
1.2	1673	0.53	0.843 0.853	0.807	0.787 0.782	0.736	1.27±0.04

As shown in this table, the agreement between the probe and optical results are in reasonable agreement with the estimated accuracy ($\pm$ 20%) anticipated from the results of the calibration phase of this study. The uncertainties listed for the ratios of probe to optical results indicate only a one standard deviation associated with the optical measurements and not those associated with temperature and concentration uncertainties and other sources of error. The results for the rich flame (ϕ=1.2) establish that the seeded-NO is being destroyed in the flame (see TASK II, Section IV, Colket et al, 1979). Moreover, the uncooled probe results are in good agreement with the optical results for the lean flame (ϕ=0.8).

III.B.2.b. Continuum Lamp Measurements

In the analysis of the data obtained with the narrow-line lamp, the results are dependent on the temperature of the emitting molecules which for the above measurements was approximately 600K. This temperature determines the width of the emission lines which must be considered in relation to the absorbing lines. An alternate emission source which provides a definable, continuum-type intensity distribution across the $Y(0,0)$ band of NO is a high pressure Xe lamp. The use of this lamp provided an independent verification of the optical results because with a high resolution spectrometer it offered single line intensity measurements and also direct line-broadening information. Its use, however, was not practical for the large combustor measurements because the high resolution spectrometer could not be exposed to the harsh environment of a test cell. This method was described in TASK I (Dodge et al, 1979) and was also employed to measure NO in these methane flames. The lines used are given in Table III-D below.

TABLE III-D

SPECTRAL LINES USED IN NO MEASUREMENTS IN
METHANE FLAT FLAMES

Group Assignmment	1	2	3	4	5	6
Line	$P_{22}(15.5)$	$Q_{22}(8.5)$	$P_{22}(16.5)$	$Q_{22}(9.5)$	$P_{22}(17.5)$	$Q_{22}(10.5)$
Identification	$Q_{12}(15.5)$	$R_{12}(8.5)$ $P_{12}(26.5)$	$Q_{12}(16.5)$	$R_{12}(9.5)$	$Q_{22}(17.5)$	$R_{12}(10.5)$

The results of these measurements are given in Table III-E. As in the case of the hollow cathode results, the deviations in the averages reflect principally the precision of the optical data. The centerline temperatures are the same as those reported for the flame stoichiometries given in Table III-C. Again, within the estimated accuracy, the results between the water-cooled probe and optical method are in good agreement. Also, good agreement was obtained with the uncooled probe for the lean flame.

III.C IFRF Burner

III.C.1 Probe Measurements

Initially, temperature profiles were measured and their dependency on burner operating conditions (i.e., swirl number, position of fuel nozzle, and design of fuel nozzle) and location within the combustor was examined. The primary objectives of these tests were to (1) find stable and repeatable operating conditions and (2) obtain reasonably flat temperature profiles in order to simplify the reduction of the optical data. The selected burner conditions are described in Section II-C. Probe locations as far downstream as practical were selected to insure that only combustion products and not un-burned or partially burned gases were sampled and that the temperature profiles were relatively flat. Six operating conditions were chosen and these are listed in Table II-B. Two swirl levels were examined and at each swirl number, three stoichiometries were tested. Although flames at lower swirl numbers were tested, these flame conditions were relatively unstable and therefore unsuitable for these experiments.

A typical temperature profile (corrected for radiation and conduction) for the run condition $\phi = 0.8$, swirl $= 1.25$, are shown in Fig. III-5. These data were taken using the aspirated thermocouple described in Section II. The dotted lines represent estimates based on measurements in the wings. The change in swirl produced no measurable difference for any of the stoichiometries. The shape of the temperature profiles for the rich and stoichiometric flames are similar to the lean flame with the centerline temperature varying according to stoichiometry (see Table III-F). In the wings, temperature measurements (uncorrected for radiation or conduction) were made using a chromel-alumel thermocouple (0.010" wire diameter) inserted through the open optical ports. The measured temperatures are much lower than are expected for adiabatic temperatures of a C_3H_8/air flame. The low temperatures observed are due to cooling from the water-cooled walls of the expansion diameter.

Stable species were measured using the SCOTT Instrument package with both the "EPA" and reference probes. No differences were observed between these probes and measured concentrations were independent of back pressure. Experimental data are listed in Table III-F and equilibrium calculations based upon

TABLE III-E

COMPARISON OF NITRIC OXIDE RESULTS OBTAINED WITH WATER-COOLED
PROBES AND CONTINUUM ULTRAVIOLET ABSORPTION: METHANE FLAT FLAMES

$\phi = 0.8$ — $[NO]_p = 1923$ ppm, Centerline (Wet) — $[NO]_p/[NO]_{op}$

Group No.	1	2	3	4	5	6	(AVE.) ($\pm 1\sigma$)
t_c	0.744	0.748	0.745	0.754	0.747	0.739	
τ_m	0.764	0.760	0.741	0.757	0.739	0.722	
$[NO]_p/[NO]_{op}$	1.10	1.05	0.98	1.01	0.97	0.93	1.01 ± 0.06

$\phi = 1.0$ — $[NO]_p = 1830$ ppm, Centerline (Wet)

Group No.	1	2	3	4	5	6	
τ_c	0.768	0.773	0.769	0.777	0.771	0.764	
τ_m	0.800	0.804	0.785	0.813	0.802	0.766	
$[NO]_p/[NO]_{op}$	1.18	1.18	1.18	1.22	1.18	1.01	1.14 ± 0.08

$\phi = 1.2$ — $[NO]_p = 1184$ ppm, Centerline (Wet)

Group No.	1	2	3	4	5	6	
τ_c	–	0.839	0.838	0.839	0.842	0.834	
τ_m	–	0.875	0.840	0.867	0.840	0.864	
$[NO]_p/[NO]_{op}$	–	1.32	1.01	1.23	0.99	1.25	1.16 ± 0.15

FIG. III-5

TEMPERATURE PROFILE ACROSS IFRF COMBUSTOR

φ = 0.8 SWIRL = 1.5

○ ELFT. = 1.3℃ Rh ASPIRATED THERMOCOUPLE PROBE
     CORRECTED FOR RADIATION AND CONDUCTION

□ BARE IN CFL THERMOCOUPLE

Figure plot: TEMPERATURE (K) versus POSITION FROM CENTERLINE (CM)
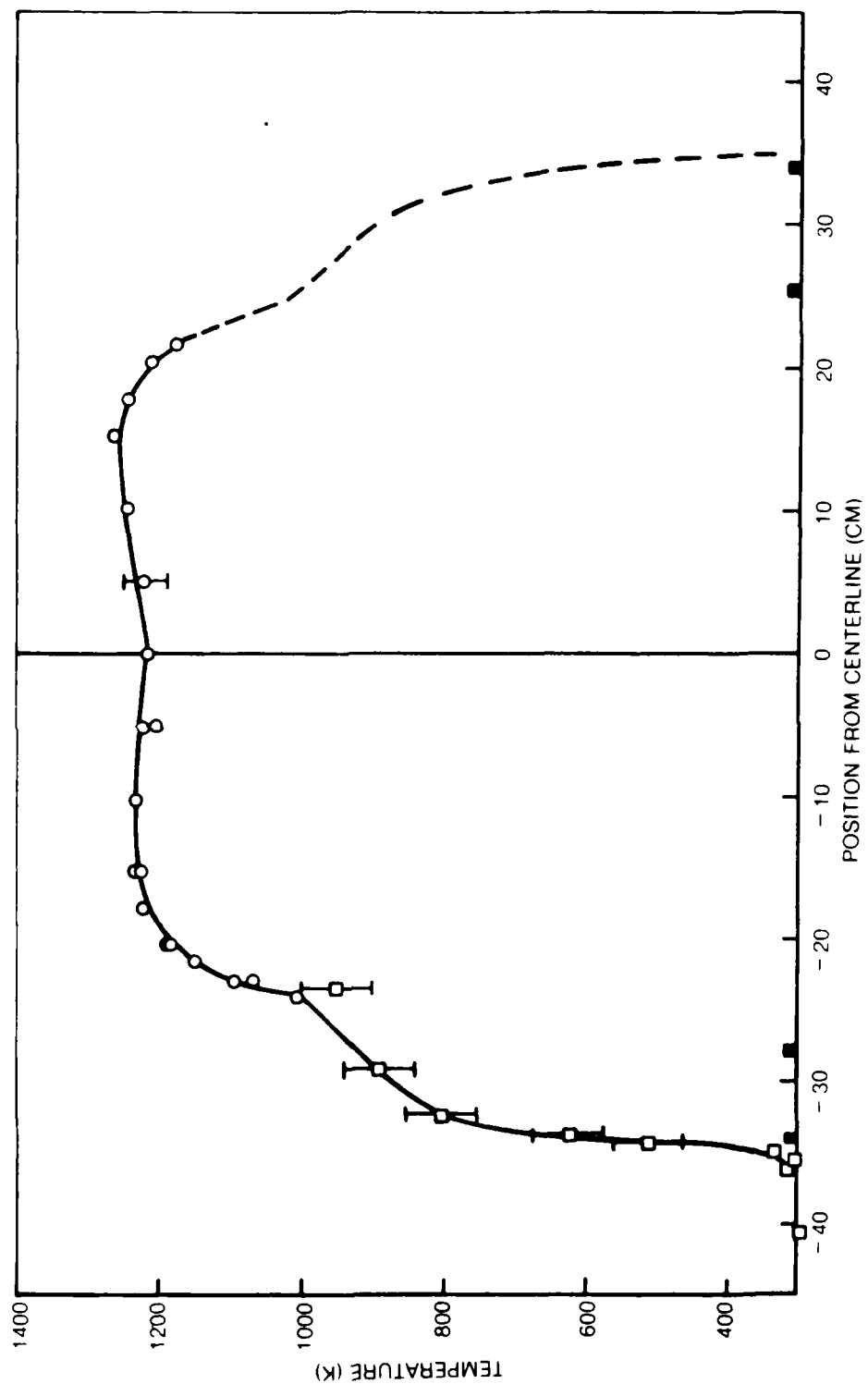
79-10-85-17

TABLE III-F

MOLE PERCENT OF STABLE SPECIES
FOR IFRF BURNER[1]
(Wet Basis)

Experimental

ϕ	O_2[2]	CO[2]	CO_2[2]	H_2O[3]	N_2[4]	Temp. (K)
0.8	4.2	9ppm[5]	8.8	11.7	75.3	1200
1.0	-	0.063[5]	10.6	15.6	73.8	1280
1.2	-	3.0	9.0	17.3	70.7	1220

Equilibrium[6]

ϕ	O_2	CO	CO_2	H_2O	N_2	Temp. (K)
0.8	3.92	<1 ppm	9.45	12.6	73.1	1200
1.0	<1 ppm	0.021	11.6	15.5	71.9	1280
1.2	<1 ppm	3.65	9.56	13.9	68.3	1220

1. Although two flames were examined (two different swirls) at each stoichiometry, measured values of these stable species were essentially the same.

2. Measured values but corrected for the presence of water vapor.

3. Water estimated from known input conditions.

4. Nitrogen calculated by difference.

5. Error ± 40% of value.

6. Based on measured temperatures.

Except where noted, the uncertainty in the experiment concentrations is approximately ± 5% of the reported value.

the measured (not the adiabatic) temperature are also given. Data for only one swirl level is given here since the data for the other swirl numbers is essentially identical. In general, agreement between equilibrium and experimental values are reasonable except for the CO_2 (and to some extent CO) values for which the measured values are about 9% low. It is believed that this difference is due to uncertainties in the fuel flow rate and/or the CO_2 calibration curve. The high estimated water value for the rich flame is due to the presence of about 3.5% molecular hydrogen (equilibrium value) and the equilibrium value of water is realistic. The presence of H_2 was not accounted for when estimating the concentration of water.

Concentrations of nitric oxide were measured to be approximately 48, 40 and 25 ppm for the ϕ = 0.8, 1.0 and 1.2 flames respectively. NO_x was typically, 4 to 5% higher than these numbers for the ϕ = 0.8 and 1.0 flames and was not measured for the rich flame. Since these levels were too low (even with the relatively long path length) to provide adequate signal-to-noise ratios in the optical measurements, nitric oxide was blended with the inlet air.

Typical profiles of nitric oxide across the optical axis and normalized to the seed concentration of NO are shown in Fig. III-6. The profile data were obtained using the 'EPA' probe and did not vary over the back pressure range examined (100-350 torr). The dotted lines are estimated extrapolations based on other similar flame measurements. Data for the other flames are quite similar. Also included on these profiles are experimental data obtained using the reference probe at two back pressures. At these conditions both the theoretical model and experimental pressure profiles inside the probe (see Task II, Colket et al, 1979) indicate that the flow in the probe is subsonic except for possibly a small region in the tip. Thus, the flow is convectively cooled. No differences between NO measurements using the reference probe and the EPA probe are observed when operating both in the convectively cooled mode. For all presssures examined and for both probes NO_x measurements were typically within 2 or 3 percent of the NO measurement. For Fig. III-6, the NO seed values for the ϕ = 0.8, 1.0 and 1.2 flames were 184, 189 and 182 ppm dry and 162, 160, and 150 ppm wet, respectively. In these calculations the 'dry' concentrations were estimated assuming the vapor pressure of water at 3 torr remained in the sample gas with a total pressure of approximately 500 torr.

Measurements were also made when supersonic flow (verified by pressure profiles) extended into the first constant area section of the reference probe. The data are reproduced in Table III-G and are compared with measurements made using the same probe but at higher back pressures, i.e., when the gases were convectively cooled. Although these data are within about 10%, there appears to be some difference between the NO measured at a low back pressure (90 torr) versus that measured at higher back pressure. In addition, the NO_{meas}/NO_{seed} ratios are smaller than those obtained at lower seed concentrations and reported in Fig. III-6. This latter result, in fact, is not surprising since the results from the flat flame burner also show a concentration dependence. The former

NORMALIZED NITRIC OXIDE PROFILES ACROSS IFRF COMBUSTOR
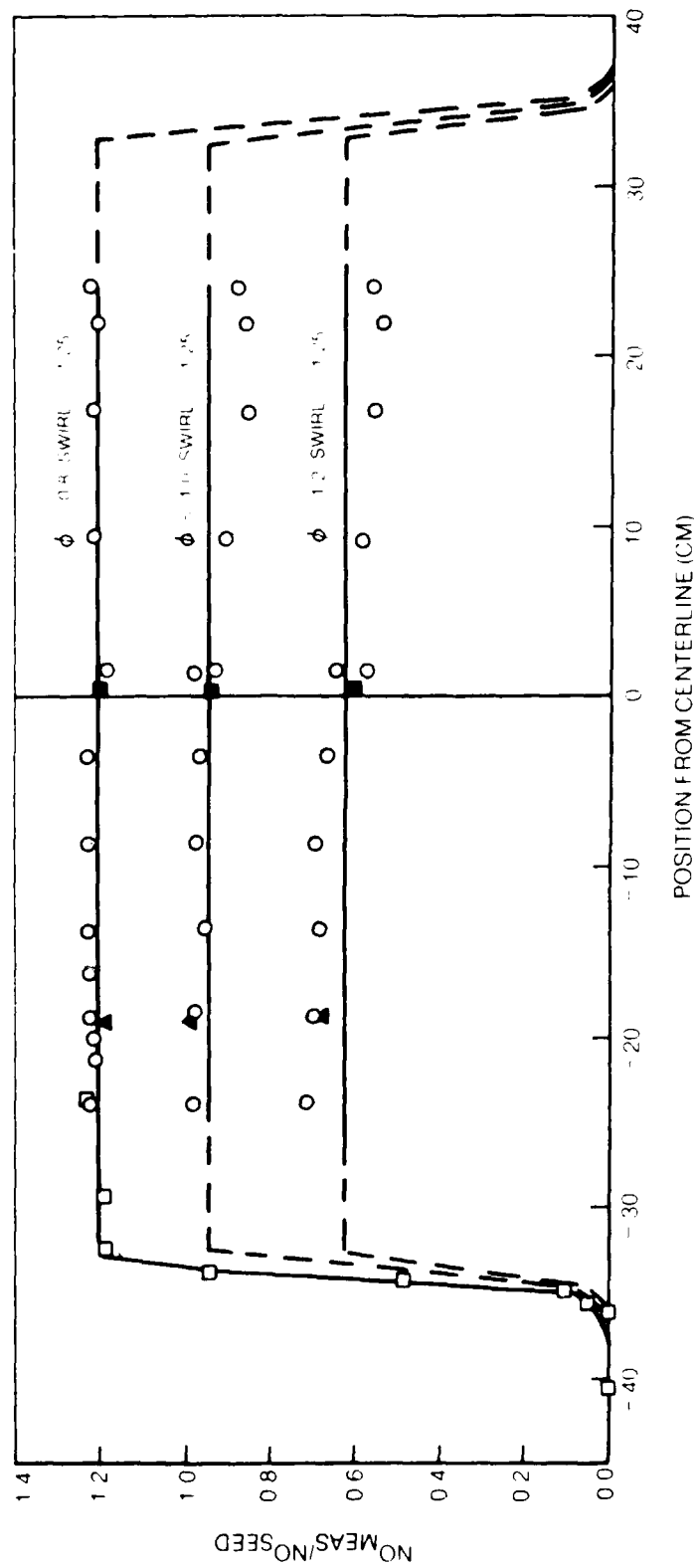
FIG III-6

79-10-85-20

TABLE III-G

COMPARISON OF NITRIC OXIDE
MEASUREMENTS USING THE REFERENCE PROBE
IFRF BURNER

	$\phi = 0.8$ Swirl = 1.25 Seed = 960 ppm	$\phi = 1.2$ Swirl = 0.63 Seed = 470 ppm	
NO (ppm)	895 ± 40	240 ± 10	Back Pressure = 190 torr
NO_x (ppm)	880	--	(0.25 atm)
NO (ppm)	--	246	Back Pressure = 380 torr (0.5 atm)
NO (ppm)	830	220	Back Pressure = 90 torr
NO_x (ppm)	820	--	(0.12 atm)

1. Supersonic flow extends into first constant area section of reference
    probe.

results apparently indicate a small difference between a probe that convectively cools and one that aerodynamically cools; however, it is more likely that the observed differences are associated with the very low operating pressure of the sampling system. For example, due to the very low pressures, the pumps could deliver only half (1 cfh) the normal flow (2 cfh) to the CLA. In either case, most of the gas was extracted with a 17.5 cfm vacuum pump immediately at the exit of the probe. Although the CLA was recalibrated to the lower flow rate, a small leak of only 2 to 3% would be difficult to detect under normal flow conditions yet would amount to a 4-6% dilution when only half the flow passed through the sample line. In addition, less water would be extracted at the refrigerator since the total pressure is lower. The resultant increase in water concentration will not only act to dilute the sample on a relative basis, but also will provide more efficient quenching of the chemiluminescent reaction and consequently decrease the response of the CLA. It is estimated that an increase in the water concentration from 1% to 3% will decrease the CLA response (due to both chemiluminescence quenching and sample dilution effects) by 4 to 5%. Consequently, it is believed that the differences observed in Table III-G are not due to differences in quenching rates of the gas sample but rather due to a decrease in sample line pressure and associated phenomena.

III.C.2 Optical Measurements

This combustor provided the higher temperature of the two large scale combustors used. Table III-H gives the optical results and compares them with those of the probes for varying stoichiometries and swirls. For the lean and stoichiometric conditions, the agreement is excellent. Again, the precision is that primarily of the optical measurement alone. The two values of τ_m for each stoichiometry represent an optical measurement at the specified combustor condition referenced to spectra obtained immediately before and after the NO seeded flame. The average signal loss on the $\gamma(3,4)$ and $\gamma(2,2)$ reference bands was 8 percent. For the conditions $\phi=1.2$, $S=1.25$, $X(NO)=103$ ppm, the agreement between probe predicted transmission and the measured transmission is only superficially good because it represents, in reality, a $\sim 40\%$ discrepancy, This is an indication of the limitation of the optical method at low concentrations and high temperatures.

III.D. FT12 Combustor

III.D.1. Probe Measurements

Three flight conditions, idle, cruise, and maximum continuous were simulated for this series of tests. The corresponding operating conditions are

TABLE III-H

COMPARISON OF NITRIC OXIDE RESULTS OBTAINED WITH WATER-COOLED PROBES AND NARROW-LINE ULTRAVIOLET ABSÓRPTION: IFRF COMBUSTOR

ϕ	Swirl	T (K)	$[NO]_p$ (centerline) ppmv	1st Bandhead τ_m	1st Bandhead τ_c	2nd Bandhead τ_m	2nd Bandhead τ_c	$\dfrac{[NO]_p}{[NO]_{nl}}$ Ave.
0.8	0.63	1200	192	0.827 0.813	0.816	0.772 0.768	0.749	1.07±0.06
1.0	0.63	1280	152	0.897 0.866	0.868	0.845 0.823	0.817	1.13±0.15
1.2	0.63	1220	103	0.924 0.924	0.903	0.894 0.900	0.864	1.32±0.05
0.8	1.25	1200	212	0.802 0.808	0.804	0.757 0.752	0.734	1.05±0.06
1.0	1.25	1280	156	0.847 0.855	0.867	0.824 0.823	0.815	0.97±0.10
1.2	1.25	1220	103	0.925 0.932	0.901	0.897 0.902	0.861	1.41±0.06
1.2	1.25	1220	135	0.882 0.861	0.872	0.845 0.819	0.822	1.04±0.11

given in Table II-C. Temperature profiles across the optical axis (same path as for the IFRF measurements) are shown in Fig. III-7 for idle and cruise conditions. These data were obtained using the Pt/Pt-13% Rh, aspirated thermocouple. The profile for maximum continuous is very similar in shape and magnitude to that for cruise. Also shown in the figure are data from a vertical profile which indicate no difference between the different quadrants. In addition to these measurements, centerline temperature measurements using coherent anti-stokes Raman spectroscopy (CARS) were made (Eckbreth, et. al, 1979). For the CARS measurements, the temperatures were 580K, 875K and 875K for the idle, cruise, and maximum continuous conditions respectively. These data agree quite well with the centerline thermocouple data obtained at the same position i.e., 590, 900 and 920K.

Measurements of CO, CO_2, and O_2 using the SCOTT instrument package and the EPA probe are listed in Table III-I. For comparison, equilibrium data based on the input conditions and measured gas temperature are also presented. Good agreement is observed between the experimental and equilibrium data except for carbon monoxide and an unexplained, high experimental value for carbon dioxide at maximum continuous. The high concentrations of CO measured behind the FT12 combustors are due to a quenching of the reaction from air dilution within the combustor. With the reference probe, the CO_2 and O_2 concentrations were not measured. Carbon monoxide concentrations were the same as with the EPA probe when the reference probe was operated both in the convective cooling mode and with supersonic flow extending into the first constant area section of the probe.

Without seed, concentrations of nitric oxide (total nitrogen oxides) on centerline were on the order of 3(15), 5(28), and 6(30) ppm for the simulated flight condition idle, cruise, and maximum continuous, respectively. These values varied as much as 20-30% from day to day for any given probe but specific variations due to probe type or back pressure were not observed. The cause of the uncertainty may be variations in input conditions for the combustor or calibration of the CLA at these low NO levels. Careful attention to obtaining accurate base line values was not given since this program focused on NO seed levels much higher than 25 ppm. In any case, it is interesting to note that the NO_2/NO ratios were typically quite high, on the order of five. The source of the NO_2 is not due to the reaction in the sample line.

$$NO + NO + O_2 \rightarrow 2 NO_2$$
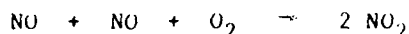
since the rate of this reaction is strongly dependent on the NO concentration and sample line pressure. Experiments with high seed values of NO (~ 800 ppm) in air at much higher sample line pressure (750 vs 180 torr) indicated only 3% conversion to NO_2. Instead, it is more likely that NO_2 is formed from NO in the combustor during the addition of relatively cold air, in the post flame region downstream of the combustor, or in the probe from the reaction with HO_2 (see TASK II Report, Section III.A.1, Colket et al, 1979). Insufficient information

TEMPERATURE PROFILE DOWNSTREAM OF FT12 COMBUSTOR

FIG III-7

79-10 85-18

III-24
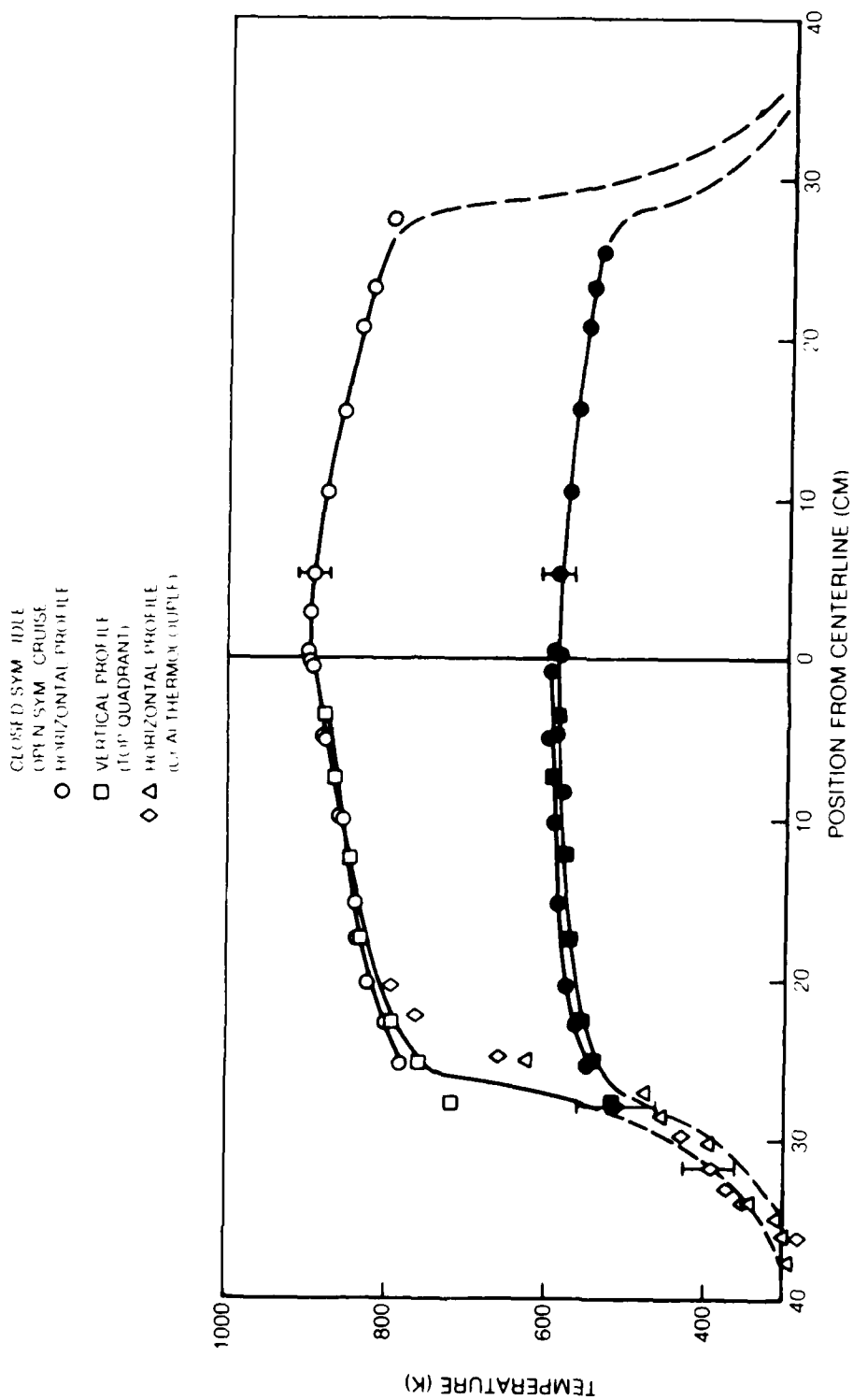
TABLE III-I

MOLE PERCENT OF STABLE SPECIES
FOR FT12 COMBUSTOR
(Wet Basis)

Experimental

	ϕ	O_2^1	CO^1	CO_2^1	H_2O^2	N_2^3	Temp. (K)
Idle	0.14	19.0	0.25	1.7	1.9	77.15	580
Cruise	0.19	16.8	0.20	2.8	2.6	77.60	870
Max. Cont.	0.20	16.5	0.17	3.3	2.7	77.33	900

Equilibrium[4]

	ϕ	O_2	CO	CO_2	H_2O	N_2	Temp. (K)
Idle	0.14	17.9	<1 ppb	1.94	1.94	77.3	580
Cruise	0.19	16.8	<1 ppb	2.60	2.58	77.0	870
Max. Cont.	0.20	16.6m	<1 ppb	2.77	2.74	77.0	900

1. Measured values but corrected for the presence of water vapor.

2. Water estimated from known input conditions.

3. Nitrogen calculated by difference.

4. Based on measured temperatures

The uncertainties in the experimental concentrations are approximately $\pm$ 5% of reported (experimental) value.

is available to determine conclusively which is the primary mechanism; however, it appears unlikely that probe reactions are responsible due to the relatively low temperature of the gas and the necessarily low radical concentrations.

Profiles of nitric oxide were obtained with seed levels of NO at 327, 326, and 326 ppm for the idle, cruise, and maximum continuous flames. Normalized profiles of nitric oxide for the idle and cruise conditions are plotted in Fig. III-8. These data were obtained using the EPA probe. Also shown are profiles of total nitrogen oxides. For maximum continuous, the centerline fraction of NO (NO_x) recovered relative to the seed value was 0.89 (1.08). In these gas samples, it is clear that there are relatively large fractions of NO_2. For example, idle conditions convert more than 40% of the total NO_x to NO_2. For the same reasons discussed in the previous paragraph, it is believed that the NO_2 is probably formed in the combustor or post flame zone rather than the probe or sampling line. Greater losses of NO are observed at idle in spite of the relatively lean stoichometry because at this level mixing is less intense and local variations in stoichiometry may be larger and may last longer than those at the other power levels. In the very fuel rich eddies, losses similar to those in the flat flame burner undoubtedly take place.

Also shown in Fig. III-8 are experimental measurements of nitric oxide using the reference probe. For most of these data the back pressure was approximately 300 torr. Although good agreement is obtained between measurements with this probe and the EPA probe, some differences are noted for one set of NO_x measurements at cruise and idle. The FT12 assembly had been removed from the test assembly and reinstalled before this second set of NO and NO_x measurements were made. Small shifts in alignment of the fuel nozzle or variations in input conditions may be responsible for the changes in NO_x recovery although no corresponding change in the gas temperature was observed.

The reference probe was also used to sample flame gases at reduced pressure (~ 95 torr) where supersonic flow conditions extended into the first constant area section of this probe. In Table III-J these values are compared to measurements taken at high back pressure with the same probe. The agreement is excellent.

III.D.2 Optical Measurements

These measurements were of particular interest in that a liquid fuel (Jet-A) was used. The agreement between the probe calculated transmission and the measured optical transmission given in Table III-K is within the expected accuracy. The precision indicated is, as previously stated, primarily that of the optical measurement. It should be mentioned that a strong continuum absorption was observed during these measurements under idle conditions. The absorption on the $Y(2,2)$ and $Y(3,4)$ reference bands was about 4 percent for the maximum continuous condition, about 14 percent for cruise, and 72 percent for idle. At the idle condition, significant quantities of hydrocarbons are present some of which absorb in this spectral region. Without the use of the signal averaging data acquisition system, the interpretation of these spectra would have been extremely difficult.

FIG. III-8

NORMALIZED NITRIC OXIDE PROFILES ACROSS OPTICAL AXIS FOR FT12 COMBUSTOR
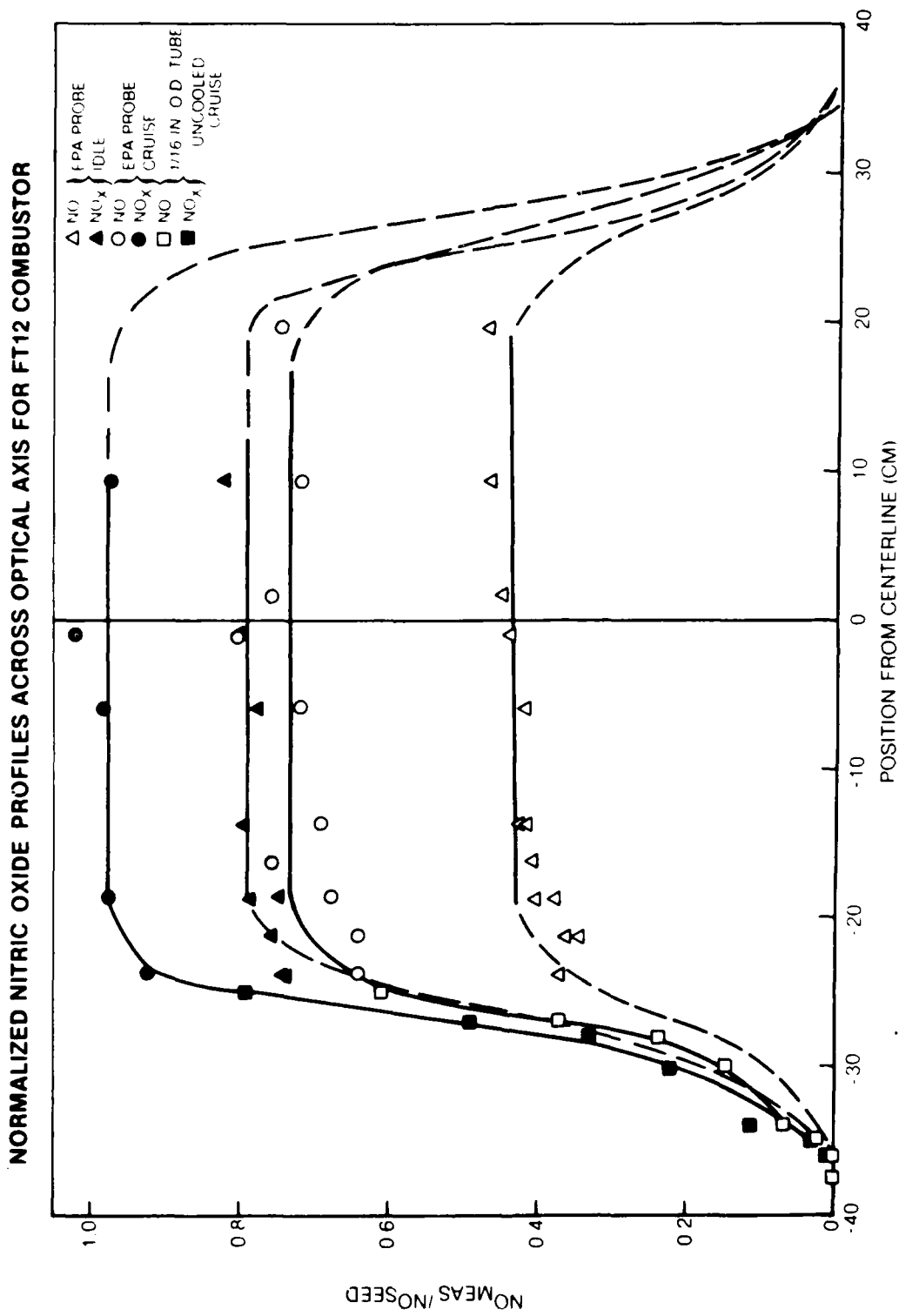
79—10—85—19

TABLE III-J
COMPARISON OF NITRIC OXIDE MEASUREMENTS USING
THE REFERENCE PROBE - FT12 COMBUSTOR

		Idle	Maximum Continuous
Back Pressure $\sim$ 205 torr (0.27 atm)	NO	395	740
	NO_x	480	800
Back Pressure[*] $\sim$ 95 torr (0.13 atm)	NO	385	740
	NO_x	478	790

* Supersonic flow extends into 1st constant area section of reference probe

TABLE III-K

COMPARISON OF NITRIC OXIDE RESULTS OBTAINED WITH WATER-COOLED PROBES
AND NARROW-LINE ULTRAVIOLET ABSORPTION: FT12 COMBUSTOR

Condition	T (K)	$[NO]_p$ (Centerline) ppmv	1st Bandhead τ_m	1st Bandhead τ_c	2nd Bandhead τ_m	2nd Bandhead τ_c	$\dfrac{[NO]_p}{[NO]_{nl}}$ (AVE)
Idle 1	580	120	0.789	0.792	0.690	0.725	$0.93^{\pm}0.0$
Idle 2	580	175	0.621	0 711	0 595	0.625	$0.82^{\pm}0.1$
						SET	$0.87^{\pm}0.1$
Cruise 1	870	240	0.750	0.755	0.697	0.680	$1.03^{\pm}0.0$
Cruise 2	870	378	0.661	0.641	0.568	0.545	$1.07^{\pm}0.0$
						SET	$1.05^{\pm}0.0$
Max. Continuous 1	900	285	0.747	0.709	0.669	0.623	$1.18^{\pm}0.0$
Max Continuous 2	900	445	0.635	0.606	0.553	0.502	$1.13^{\pm}0.0$
						SET	$1.16^{\pm}0.0$

IV. DISCUSSION

IV.A. Introduction

As noted in the introduction to this report, the discrepancies between optical and probe measurements, reported by W. K. McGregor, J. D. Few, M. G. Davis, and their colleagues between 1973 and 1976, ranged from factors of 1.5 to 6.0. It was these large discrepancies that stimulated this study; therefore, it is important to consider the results of the present study in context with their original work. As this study was being performed, two other separate investigations of this problem were being conducted by independent research groups. The results of this study will also be considered relative to those two investigations.

IV.B. Comparison of Optical and Probe Results (TASK III)

It is possible to summarize the results of this task in the following manner. For the exhaust gas measurements made by UTRC, deviations between optical and probe results were generally less than 25%. Frequently, the probe measured NO values were greater than those measured optically. Measurements were made in turbulent and non-turbulent media and at temperatures up to $\sim$1900K. The combustion systems were fired with both gaseous and liquid fuels. Based on the observations of the calibration phase of this study (TASK I), it had been estimated that an accuracy of $\pm$20% could be anticipated. If it is assumed that precision is related to accuracy, then the agreement between the optical and probe measurements of NO in TASK III is within that projected 20% accuracy. The accuracy is estimated from the accumulation of uncertainties associated with: (1) the resetability of the combustors; (2) temperature measurements and corrections; (3) spatial distribution of temperature and pressure along the optical path; (4) continuum type absorption due to particulates and molecular species other than NO; (5) lamp drift; (6) beam steering; (7) perturbations in temperature and flow by probes; (8) sample quenching; (9) sample transfer; (10) calibration standards; and (11) the chemiluminescent analysis method. Moreover, the results of the infrared measurements given in Appendix A, within the scatter of that instrument's output, are in good agreement with the results of the probe measurements. Hence, large discrepancies between optical and probe results like those noted earlier have not been observed. Although the bulk of the measurements were made with metallic water-cooled probes, the measurements made with an uncooled metallic probe on the flat flame burner were also in good agreement with the optical measurements when oxygen was present, i.e., in an overall lean condition.

As shown in TASK I Report (Dodge et al, 1979), the characteristics of the capillary discharge lamp used in the original work are similar to the hollow

cathode lamp used in this study. Also noted in the above report was the fact
that the model used to reduce the original data was in serious error. That
model (ARO) has been subsequently corrected and has been briefly described
by Few et al (1979). The new ARO model is similar to that used by UTRC to
reduce its data; however, deviation at elevated temperatures is expected
because the UTRC model uses Weisskopf broadening theory while that of ARO uses
Lorentz theory. Nevertheless, preliminary data reduction of the ARO optical
data indicated an agreement of 30% between optical and probe results (J. Few,
private communication). It is expected that these results will be published
separately.

IV.C.   Recent Related Studies

The paper published by Meinel and Krause (1978) duely noted that a major
discrepancy had been observed between ultraviolet and probe measurements of
NO by ARO personnel. Also noted was the fact that the infrared gas correla-
tion measurements of Gryvnak and Burch (1976a, b) indicated discrepancies of ∿30%
versus factors of 1.5 to 5. In their study, Meinel and Krauss used a differen-
tial resonant line (narrow-line) absorption technique in the ultraviolet to
monitor NO in hydrogen-air and propane-air flames. The temperatures of these
flames covered the range from 1700K to 2500K. The differential measurement
technique was employed to compensate for the continuum absorption due to O_2
and CO_2. The probe used was water-cooled quartz. For both flame systems,
the agreement between probe and optical measurements was within 20-30%. The
agreement was best for the lean conditions up to ϕ =0.9. The deviations were
the greatest at stoichiometric conditions, i.e., ϕ =1.0. The excellent agreement
reported under lean conditions is consistent with the results given in Section
III of this report. Where the deviations were greatest, it was the optical
method which yielded the lower NO concentrations. Nevertheless, no major
discrepancies comparable to the original ARO work were observed.

A more recent study by Falcone, Hanson, and Kruger (1979) used an infra-
red tunable diode laser to measure NO (5.2μm) in the postflame gases of a
flat flame burner. Methane/air flames seeded with NO were probed with an
uncooled quartz probe. The seed levels ranged from ∿100 ppm to 2000 ppm and
peak temperatures were approximately 1900K. After correcting their data for
the collisional quenching effect of H_2O (wet sample gas) on their chemi-
luminescent analyzer calibration, they report that the infrared measurement
was typically 20% higher than both the probe and seed values. At low concen-
trations, this might be expected due to the production of thermal NO in the
flame; however, this is not true at high seed levels. They estimate 5% uncer-
tainty due to inhomogeneities in the optical path and maintain 15% uncertainty
is unexplained; but, they did not discuss some of the other pertinent sources
of uncertainty which are given at the beginning of this section. The reported
destruction of NO in the rich flames is similar to that observed in TASK II

and TASK III. Finally, their measurements were consistent with those reported by Gryvnak and Burch (1976a, b), the results of this (UTRC) study, and do not show major discrepancies.

IV.D. Original Studies: Comments

The demonstration that in situ measurements were feasible in the hostile environments of jet combustor and engines was a significant achievement. Moreover, the development of a first principles model to interpret optical data in inhomogeneous media such as jet exhausts was an excellent approach to a difficult problem. The first reported work was obtained during CIAP by McGregor et al (1972) and was compared with probe data obtained by Neely and Davidson (1972) and Grissom (1972). However, this work cannot be used to establish that there is a fundamental problem with properly made probe measurements of NO. The principal reason for this is that those optical data were not reduced with a first principles model but with a room temperature calibration curve. Moreover, no attempt was made to use a zonal treatment of the inhomogeneities in temperature, pressure, and concentration. Other difficulties include the misconception that collisional broadening is much less than Doppler broadening, a major underestimation of the influence of the inhomogenities on the accuracy of the optical method, the possibility of a stagnation zone in front of the probe, and the wrong probe design for sampling the fuel laden exhaust in the maximum afterburning conditions.

The first report describing the first principles model was that of McGregor et al (1973). Unfortunately, this report and as well as other reports on model verification (e.g. Davis et al, 1975) contain serious spectroscopic problems. These problems are listed in detail in TASK I Report and are sumarized in Section V of this report. Because it was stated in these reports that good agreement existed between the predictions of a faulty model and experimental data, there is evidence to suggest that the experimental data had serious errors. An example of this is contained in Table IV-A where ARO calibration data obtained under ideal conditions are compared with old and new model predictions. Since the transmissions predicted by new ARO and UTRC models are in agreement and have been verified, then a problem exists in the measurement of transmission or in the measurement of mole fraction or pressure. Possible sources of error could be nonlinear optical and electronic detection, faulty gas mixing procedures, and inexact chemiluminescent calibration.

The combustor work which followed the CIAP measurements was that involving the AVCO-Lycoming research combustor. These measurements were made on a super- sonic exhaust stream and, hence, can only be related to the results of Section III in an indirect way. Nevertheless, there are some points which should be considered. Few et al (1975) indicated that discrepancies between optical and probe NO concentrations with the optical values higher by factors of 3.5 to

TABLE IV-A

A COMPARISON OF CORRECTED MODEL RESULTS WITH ORIGINAL
MODEL AND VERIFYING EXPERIMENTAL RESULTS: AN EXAMPLE

(Data From AEDC-TR-76-12, Davis et al (1976), Fig. 9)

Temperature = 422K
$n[NO] = 1.31 \times 10^{15}/cm^3$
Pathlength = 91.4 cm   2nd Bandhead Transmission

Curve No.	P (atm)	$[NO]_p$ (ppm)	Meas.	Orig. ARO Model (6/78)	New ARO Model (6/79)	UTRC Model (6/79)	Discrepancy* (ARO Orig. to
1	1.36	55	0.820	0.824	0.690	0.690	1.92
3	0.71	106	0.710	0.737	0.598	0.598	1.68
5	0.19	395	0.467	0.549	0.414	0.429	1.47

*Discrepancy = $\ln\tau_{New}/\ln\tau_{Orig}$

6.0. As evidence indicating that NO was being destroyed in the probe, results of optical measurements made in the sample line were presented which indicated agreement between the chemiluminescent analyzer and the ultraviolet technique. This agreement, however, is inconsistent with the fact that the model that was used to process the optical data was in error. This again suggests experimental difficulties similar to those discussed above and indicated in Table IV-A. (Falcone et al (1979) discuss some problems encountered in making chemiluminescent analyses of wet samples and comparing them with infrared results.) In the reduction of their data, Few et al (1975) did not employ a zonal treatment of the NO and temperature profiles. From the data presented, the probe measurements were sparse. In fact, neither experimental NO concentration data were obtained in the region beyond the width of the nozzle nor were temperature measurements made. Static temperature, static pressure, and optical path were predicted rather than actually measured. However, the placement of a probe in a supersonic flow 0.5 inches downstream of an exhaust nozzle can cause a major perturbation to the flow and temperature. Also, as noted in TASK II Report (Colket et al, 1979), a stagnation zone in front of their turbular inlet probe could perturb the gas samples. For air at a Mach number of 1.15, a 25% rise in temperature can be produced. For this type of probe, the gas must decelerate to a low Mach number at the entrance, and consequently stagnation temperatures will be approached even if an external stagnation zone does not exist. This evidence indicates that not only were there difficulties with the optical measurements, but most likely proper probe technique was not employed, i.e., 50% pressure drop occuring at the probe orifice as required by the Federal Register. Consequently, these measurements cannot be used to establish a fundamental problem with the probe technique either in subsonic or supersonic flows.

Following the AVCO-Lycoming measurements, ultraviolet and infrared measurements were made on the T-56 combustor exhaust by Few et al (1976) and Grvynak and Burch (1976a, b), respectively. As mentioned earlier, the infrared measurements show discrepancies of 20-30% with the probe measurements. This was the first time that a proper comparison of probe and optical data was performed, i.e., a zonal treatment accounting for temperature and concentration nonuniformities along the optical path. The ultraviolet data processed in the same manner indicated discrepancies of 1.5 to 1.9 with the probe data. However, these data were processed with a faulty model. Table IV-B gives the results reprocessed with a correct model. The discrepancies are 30% or less and the average error is less than 20% with the optical method measuring more NO. With the uncertainties in these measurements, this can be considered good agreement, hence, a fundamental problem with the probe method has not been established by these measurements.

TABLE IV-B

T-56 MEASUREMENTS BY ARO REEXAMINED WITH
CORRECTED SPECTRAL MODEL

(From Table 3, AIAA Paper 76-109)

2nd Bandhead Transmission

Run Number	Location Downstream	Pyridine Added	Calculated from Probe Values τ_c	Meas. τ_m	$\dfrac{[NO]_p}{[NO]_{nl}}$*
1a	3		0.909	0.884	0.77
1b	3	x	0.895	0.875	0.83
1c	3	x	0.882	0.850	0.78
1d	3	x	0.875	0.830	0.72
2	18		0.881	0.874	0.95

*$\ln\tau_c / \ln\tau_m$

V. SUMMARY AND CONCLUSION

Since this is the last in this series of reports on the measurement of NO by optical and probe methods, it is appropriate to include the conclusions of the first two parts of the study along with those of this the third part so that the conclusions for the complete study can be viewed in their entirety.

V.A Optical Calibration (TASK I)

In the first part of the study on optical calibration (Dodge et al, 1979), it was concluded that known amounts of NO can be provided for calibration purposes at temperatures ranging from 300 K to 2000 K if certain procedures are used. For temperatures up to 850 K, NO diluted in N_2 and Ar will not significantly ($< 10\%$) decompose when flowed through a quartz-bed heat exchanger. Although it was not experimentally verified, a kinetic analysis indicated that substantial decomposition would not occur in this exchanger up to 1000 K. For temperatures of 1000 K to 2000 K, NO seeded into a lean $H_2/O_2/Ar$ flat flame is recovered in the post flame region. Detailed temperature and concentration distributions along the optical path were obtained with thermocouples and probes. For the highest temperatures, the thermocouple data were corrected for radiation losses. At the low temperatures (≤ 850), the concentration measurements were made with both uncooled quartz and metallic probes. The concentration measurements downstream of the flat flame burner were obtained with water-cooled quartz probes. The NO analysis was performed on-line by chemiluminescence and mass spectroscopy.

At the beginning of this study, a detailed spectroscopic computer model was provided by ARO, Inc. This model had been used by several authors at ARO (McGregor et al, 1973; Few et al, 1975; Davis et al, 1976) who pointed out serious discrepancies between probe and optical NO concentrations measured under similar conditions. A detailed review of the spectroscopic theory upon which the model was based indicated several significant errors. A complete description of these errors, along with where these errors exist in previously published reports and literature, is given in Appendix B of TASK I Report (Dodge et al, 1979). However, these errors can be summarized by the following. First, the equation relating the oscillator strength for an individual line to band oscillator strength was in error by a factor of 4. Second, the equation relating the number density of an individual state to the total number density was in error by a factor of 2. Third, originally no distinction in population was made between the $^2\pi_{1/2}$ and $^2\pi_{3/2}$ states. This was partially corrected in the later work, but without correct normalization. Fourth, an error in the Honl-London factor for the Q_{11} lines was present in the program supplied at the beginning of this study. Fifth, the equation which relates broadening parameter

to collision cross section was in error by an order of magnitude. Other minor
errors and suggested improvements are also given in the above appendix.
Because of these errors, the results of the optical measurements were not
reliable and, hence, cannot be used to establish a discrepancy between NO
concentrations determined with probe and optical methods.

The spectral theory was corrected and incorporated into a new computer
model. This model was used to process both high resolution, single line data
obtained with a continuum lamp and low-resolution data obtained with a narrow-
line lamp. Since the results from these two different optical methods were
self-consistent, the validity of the model was established.

Two of the required inputs for the model are broadening parameter and
oscillator strength. Broadening parameters for NO in Ar, N_2, CO_2, and CH_4
were measured by the direct observation of isolated absorption lines. For the
majority of the data, the resolution was sufficiently high (full width at half
maxima < 0.0020 nm) that the contribution of the slit function to the total
line shape was minimal. The broadening of NO in H_2O at elevated temperatures
was inferred from $H_2/O_2/Ar/NO$ flame measurements. The temperature dependence
of the broadening parameters did not appear to follow the Lorentz broadening
theory at elevated temperature but that of Weiskopf. Oscillator strengths were
also determined from these same high resolution spectra. The broadening results
are unique; the oscillator strengths are in excellent agreement with the latest
recommended value. Moreover, oscillator strengths were determined from low
resolution using the broadening parameters determined in high resolution. With
proper accounting for emission lines present in the lamp output but not due to
NO, these strengths were in good agreement with recommended values.

Sufficient measurements were conducted and compared with model predictions
of absorption to conclude that the ultraviolet optical system based on the
hollow cathode lamp is calibrated to measure NO. In addition, similar measure-
ments were made with the capillary discharge lamp. Those measurements are
reported in TMR-79-P7 (Few et al, 1979) and TR-79-65 (Few et al, 1979).

Finally, an empirical calibration of the infrared gas correlation
spectrometer was performed (Appendix A). Because this instrument was origin-
ally designed for stack monitoring, i.e., low temperatures and high densities,
it was not well-suited for the measurements of interest here. The low temper-
ature data indicated that the instrument was 20 percent more sensitive relative
to the calibration previously used in jet combustor measurements. This varia-
tion is attributed to changes in grating alignment. A dependence of the cali-
bration on broadening gas was observed and determined. For temperatures up
to 900 K, the calibration, within the scatter of the instrument output, remained
constant. Above 900 K, a significant decrease in sensitivity was observed.
This dependence is most likely due to significant changes in the populations of

the lines selected by the grating assembly. However, sufficient data were obtained to allow measurements to be made at high temperatures if high NO seeding of the media is used.

V.B   Probe Method (TASK II)

The major conclusions of TASK II are the following. First, water-cooled quartz, stainless steel, and copper-tipped miniprobes yield the same NO concentrations when sampling products from methane/oxygen/ nitrogen flames with seeded NO at temperatures up to 2000 K and irrespective of stoichiometry. This similarity in behavior occurs over a wide range of probe back pressures; hence, no advantage is gained from back pressures less than 0.5 atm when sampling atmospheric pressure flames.

Second, uncooled stainless steel probes give NO concentrations somewhat lower (10-15%) than the cooled probes mentioned above for lean methane/oxygen/ nitrogen flames. For stoichiometric and rich flames, the NO concentrations are significantly less and for rich flames, the amount of loss is dependent on probe back pressure. The destruction of NO in this uncooled probe is similar to that encountered in NO/NO_2 converters operated in the absence of oxygen. Hence, uncooled stainless steel probes are only suitable for sampling NO in the presence of oxygen.

Third, in general, for miniprobes and microprobes, aerodynamic quenching is not possible because of fluid mechanical and geometric constraints. However, rapid-cooling of the sample gases (within a few milliseconds) can be achieved by convective heat transfer to the probe walls.

Fourth, for microprobes, mass flow measurements indicate that in the sampling of high temperature gases choked flow does not occur at the classical pressure ratio. This result was predicted by the probe model and suggests that quenching processes may be less efficient than those estimated in previous studies. A kinetic analysis indicates that quenching rates are still sufficiently rapid for sampling NO in exhaust gases; however, the impact of slower quenching rates on gases sampled from reactive flame zones may have to be examined.

Fifth, unlike the small scale probes, it is possible to construct a large scale water-cooled probe that can produce aerodynamic quenching of the sample; however, measurements made on both gaseous and liquid fueled combustion systems yielded essentially the same results regardless of the quenching mode, i.e., aerodynamic or convective. Given this fact plus the complexity of probe construction and the difficulties in achieving the low probe back pressures required of the aerodynamic mode, there is no advantage to aerodynamic quenching in the measurement of NO.

Sixth, the model predictions of pressure distribution and mass flow within the large scale probe agreed well with the experimental data. In addition, the model accurately predicted that the microprobe would not choke at the classical pressure ratio when sampling at high temperatures. Based on these results, it can be stated that the fluid dynamic and heat transfer processes have been adequately described in the model for the case of fluid mechanical choking at the probe orifice.

Seventh, a kinetics analysis of gas phase reactions known to destroy NO indicated that no significant loss of NO would occur during the sampling process if the sample temperature was reduced to 1000 K in approximately 1-2 milliseconds. The results of this study are consistent with this analysis.

Eighth, a review of the literature indicated no definitive study where large differences (> 20%) between measurements of nitrogen oxides from different probes were observed when properly designed probes and sampling lines were used and correct calibration of the chemiluminescent analyzer was performed. A properly designed probe is one that does not perturb the flame environment, does not stagnate the flow, is water-cooled, operates at a back pressure to external static pressure ratio low enough to aid in quenching of reactions, and finally has hot walls (> 600 K) which are limited only to the front portion of the tip such that the local gas residence time is on the order of 10 microseconds or less. Proper sampling lines are those in which the residence times are short relative to the time required for the conversion of NO to NO_2 and the loss of NO_x in water traps and particulate filters. Correct calibration of the chemiluminescent analyzer consists of accounting for the influence of gases other than N_2 on the introduction of NO into the chemiluminescent reaction chamber and the collisional deactivation of excited NO_2.

V.C Comparison of Probe and Optical Methods (TASK III)

From the third part of this study, the following conclusions can be drawn.

First, NO concentrations determined in subsonic exhaust streams by narrow-line ultraviolet spectroscopy are in good agreement ($\pm$ 20% or better) with those determined with water-cooled probes. This agreement was observed for a wide range of conditions when the optical data were processed correctly and the probe sampling was conducted properly. These conditions included temperatures from 293 K to 2000 K, and both turbulent and nonturbulent flow. Proper processing of the optical data entails a detailed knowledge of temperature and pressure along the optical path, adequate characterization of the lamp, and a correct spectral model. Proper probe sampling consists of rapidly quenching the gas sample by sudden pressure reduction and convective cooling, rapid sample transfer, especially in the presence of oxygen, and a calibration procedure for the chemiluminescent analyzer that includes viscous and

collisional deactivation effects. Moreover, this agreement was seen irrespective of probe material (metallic or quartz) and fuel type, i.e., gaseous or liquid.

Second, good agreement between optical results and uncooled probes was observed with measurements made in exhaust streams where oxygen is present, i.e., overall lean systems. However, in rich stoichiometric and systems, uncooled metallic probes gave NO concentrations which were in substantial error (> 100%) and, hence, cannot be employed for measurements except in overall lean systems.

Third, the infrared correlation spectroscopic measurements can be considered, within the scatter, in good agreement with the water-cooled probe measurements.

Fourth, recent studies involving the measurement of NO in flat flame exhausts are in good agreement with the results of this study. These studies were made by a narrow-line ultraviolet method (Meinel and Krauss, 1978) and by an infrared laser technique (Falcone et al, 1979).

Fifth, to reiterate the conclusion of Section V.B, there is no advantage gained in operating a probe in an aerodynamic quench mode while measuring NO.

Sixth, in the measurement of NO in exhaust streams, the optical methods, although nonperturbing, offer no major advantage over probe methods. The nonperturbing aspect is offset by the facts that: (1) the optical path in an unconfined exhaust stream is most easily defined by a probe method; and (2) static temperature and pressure distributions are necessary to reduce the optical data, yet presently, have to be determined by probe methods. Moreover, to improve the sensitivity of the optical absorption method at high temperatures (> 1000 K), low pressures (< 0.2 atm) and short pathlengths, multiple pass optical systems are required.

Finally, the previously published ARO ultraviolet measurements cannot be used to deduce that major fundamental discrepancy (50%) exists between probe and optical results in subsonic flows. Serious problems were identified in the spectroscopic model. Subsonic data when reprocessed did not indicate a major discrepancy. These same problems were present when the optical data obtained on supersonic flow were processed and, hence, no conclusion can be drawn for the supersonic flow. Moreover, there is evidence to suggest that probe measurements made in the supersonic flows are questionable along with the method used to compare the optical and probe results.

REFERENCES

Beer, J. M. and N. A. Chigier: Combustion Aerodynamics, ed. by J. M. Beer, John Wiley and Sons, Inc., New York, 1972.

Benson R. and G. S. Samuelsen: Presentations at the Western State Section of the Combustion Institute, Fall Meeting, Paper No. 76-39, October 18-20, 1976 and Spring Meeting, Paper No. 77-7, April 18-19, 1977.

Benson, R., G. S. Samuelsen and R. E. Peck: Presentation at the Spring Meeting Western State Section of the Combustion Institute, Paper No. 76-11, April 19-20, 1976.

Colket, M. B., M. F. Zabielski, L. J. Chiappetta, L. G. Dodge, R. N. Guile, and D. J. Seery: Nitric Oxide Measurement Study: Probe Methods. Report prepared for DOT/FAA under Contract No. FA77WA-4081, UTRC R79-994150-2, November 1979.

CIAP (Climatic Impact Assessment Program) DOT-TST-75-51, 52 (1975).

COMESA (Committee on Meteorological Effects of Stratospheric Aircraft) U.K., Meteorological Office, Bracknell (1975).

COVOS (Comite d'Edudes sur les Consequences des Vols Stratospheriques) Societe Meteorologique de France, Boulogne (1976).

Crutzen, P. J.: Quart. J. Royal Met. Soc., 96, 320 (1970).

Crutzen, P. J.: Ambio, 1, 41 (1972).

Davis, M. G., W. K. McGregor and J. D. Few: Arnold Engineering Development Center Report AEDC-TR-74-124 (AD-A004105), (1976 a).

Davis, M. G., J. D. Few and W. K. McGregor: Arnold Engineering Development Center Report AEDC-TR-76-12 (AD-A021061), (1976 b).

Davis, M. G., W. K. McGregor, and J. D. Few, J. Quant. Spectrosc. Radiat. Transfer, 16, 1109 (1976).

Dodge, L. G., M. B. Colket, M. F. Zabielski, J. Dusek and D. J. Seery: Nitric Oxide Measurement Study: Optical Calibration. Report prepared for DOT/FAA under Contract NO. FA77WA-4081, UTRC R79-994150-1, April 1979.

Eckbreth, A. C., P. A. Bonczyk and J. F. Verdieck: Investigations of CARS and Laser-Induced Saturated Fluorescence for Practical Combustion Diagnosis. Final Report under EPA Contract 68-02-3105, United Technologies Research Center R79-954403-13, September, 1979.

REFERENCES (Cont'd)

England, C., J. Houseman and D. P. Teixeira: Combustion and Flame 20, p. 439, (1973).

Falcone, P. K., R. K. Hanson, and C. H Kruger: Paper No. 79-53 presented at the Western States Section of the Combustion Institute, October 1979.

Federal Register, Vol. 37, No. 239(2) - EPA, Aircraft and Aircraft Engines, Proposed Standards for Control of Aircraft Pollution, December 12, 1972.

Federal Register, Vol. 41, No. 181, Part 87 - Control of Air Pollution from Aircraft and Aircraft Engines, September 16, 1976.

Few, J. D., R. J. Bryson, W. K. McGregor, and M. G. Davis, in Proc. Intl. Conf. Environmental Sensing and Assessment, Las Vegas, Nev. (Sept. 1975).

Few, J. D., W. K. McGregor, and H. N. Glassman, Ultraviolet Spectral Absorption Measurements of Nitric Oxide Concentration in T-56 Combustor Exhaust, AIAA Paper No. 76-109, AIAA 14th Aerospace Sciences Meeting, Washington, DC, January 26-28, 1976.

Few, J. D., W. K. McGregor, and H. N. Glassman, Resonance Absorption Measurements of NO Concentration in Combustor Exhaust, in Experimental Diagnostics in Gas Phase Combustion Systems, edited by B. T. Zinn, p. 187, AIAA, 1977.

Few, J. D., R. J. Bryson, and W. K. McGregor: Arnold Engineering Development Center Report AEDC-TR-76-180 (1977).

Few, J. D., H. S. Lowry III, W. K. McGregor and D. R. Keefer: Interagency NO Measurement Investigation, Phase I: AEDC Results, AEDC-TMR-79-P7, July 1979.

Few, J. D., H. S. Lowry III, W. K. McGregor, and D. R. Keefer: Interagency Nitric Oxide Measurement Investigation: AEDC Results for Phase I (Calibration Technique for Optical Measurement System), AEDC-TR-79-65, October 1979.

Fristrom, R. M. and A. A. Westenberg: Flame Structure, McGraw-Hill, New York, 1965.

Glawe, G. E., F. S. Simmons, and T. M. Stickney: NACA TN 3766 (1956).

Gordon, S. and B. J. McBride: Computer Program for Calculation of Complex Chemical Equilibrium Compositions, Rocket Performance, Incident and Reflected Shocks, and Chapman-Jouquet Detonations. NASA SP-273 (1971).

Grissom, J. L.: Proc. Second Conf. Climatic Impact Assessment Program, p. 199, Cambridge, Mass, (November 1972).

REFERENCES (Cont'd)

Gryvnak, D. A., and D. E. Burch: AFAPL-TR-75-101, (1976a).

Gryvnak, D. A., and D. E. Burch: AIAA Fourteenth Aerospace Meeting, AIAA No. 76-110, Washington, D. C., (1976b).

Johnston, H. S: Science, 173, 517.

Land, T. and R. Barber: Transacting of the Society of Instrument Technology, 6, 112 (1954).

McCullough, R. W., C. H. Kruger and R. K. Hanson: Comb. Sci. Tech., 15, 213-223 (1977).

McGregor, W. K., J. D. Few and C. D. Litton: Arnold Engineering Development Center Report AEDC-TR-73-182, AD-771 642 (1973).

McGregor, W. K., B. L. Seiber and J. D. Few: Proc. Second Conf. Climatic Impact Assessment Program, p. 214, Cambridge, Mass. (November 1972).

Meinel, H.: Z. Naturforsch., 30a, 323 (1975).

Meinel, H. and L. Krauss: Combustion and Flame, 33, 69 (1978).

NAS (National Academy of Science), "Environmental Impact of Stratospheric Flight", Climatic Impact Committee (1975).

Neely, J. and D. L. Davidson: Proc. Second Conf. Climatic Impact Assessment Program, p. 180, Cambridge, Mass., (November 1972).

Oliver, R. C., E. Baver and Wasylkiwskyj: DOT-FAA Rpt. FAA-AEE-78-24.

Oliver, R. C., E. Baver, H. Hidalgo, K. A. Gardner and Wasylkiwskyj: DOT-FAA Rpt. FAA-EQ-77-3 (1977).

Seery, D. J. and M. F. Zabielski: unpublished.

Vranos, A., B. A. Knight, J. J. Sangiovanni, L. R. Boedeker, and D. J. Seery: Feasibility Testing of Micronized Coal-Oil (MICO) Fuel in a Model Gas Turbine Combustor, UTRC R79-954451-1, May 1979.

Appendix A

Measuring NO In Aircraft Jet
Exhausts By Gas-Filter Correlation
Techniques, Task III

David A. Gryvnak

Ford Aerospace and Communications Corp.
Aeronutronic Division
Ford Road
Newport Beach, California   92663

September 1979

FINAL REPORT TASK III

INTRODUCTION AND SUMMARY

Tests were conducted using the smokestack instrument described in the Task I report to measure the amount of NO under four controlled test conditions. The first were a series of tests performed, both at Ford Aerospace and Communications Corp (FACC) and at United Technologies Research Center (UTRC) using static cells of 10 cm and 20 cm long respectively with the NO samples at room temperature. A second set of tests at UTRC were performed using a Flat Flame Burner at approximately 1850 K with a path length of 17.5 cm. A third set of tests were performed using an IFRF burner, the sample being at approximately 1300 K with a pathlength of 67.3 cm. The fourth set of tests were performed using an FT12 burner can, here three different power conditions were used so that the sample temperature varied from 600 to 900 K. The pathlength was 67.3 cm. Three different stoichiometric conditions were used for the IFRF and FT12 burner tests, $\phi = 0.8$, 1.0 and 1.2, lean to rich. In addition, during the IFRF tests the exhaust had a tangential velocity imparted to it by vanes that were inside the burner assembly. These vanes were changed so that two different tangential velocity conditions were tested, swirl = 0.63 and 1.25. The amounts of NO determined using the smokestack instrument were compared to the amounts determined using the probe instrument.

The results of Task I predicted that the values obtained by the smokestack instrument would be higher than the probe results for temperatures below 900 K and lower for temperatures above 900 K. The results of the tests in Task III are in good agreement with the results of Task I. Also theoretical calculations were made with the use of a computer, simulating the response of the smokestack instrument and the results are in agreement with the values obtained by the smokestack instrument. These calculations indicate that the smokestack instrument is correctly responding to the amount of NO in the different burners at the higher temperatures and that the probe results are quite good.

DATA REDUCTION

The probe data and the data from the smokestack instrument were reduced in a manner as described in the Task I report. For a sample at constant temperature and concentration, the absorber thickness u is related to the temperature, θ, pathlength L and pressure, p, of a sample in the following manner.

$$u(\text{molecules/cm}^2) = \frac{p(\text{atm})\ L(\text{cm})}{\theta(K)}\ 7.34 \times 10^{21}. \tag{1}$$

For a sample that has temperature and concentration gradients over a pathlength L, the absorber thickness can be found from the integrated values.

$$u = 7.34 \times 10^{15}\ C\Delta L\sum_i\ \frac{M_i}{\theta_i}, \tag{2}$$

where

ΔL = incremental pathlength, $\sum_i \Delta L = L$,

C = centerline concentration (ppm),

M_i = molar concentration for i^{th} increment,

θ_i = temperature (K) of ith increment.

$\Delta L = 0.5$ was used for the Flat Flame Burner results, and

$\Delta L = 1.0$ was used for the IFRF and FT12 Burner results.

The temperature profiles and molar concentration profiles that were supplied by UTRC for the different burners and their associated stoichiometric and swirl conditions are shown in Figs. 1 through 8. These are the profiles used to determine the absorber thickness for the probe results, denoted as uc.

The values determined by the smokestack instrument, denoted as um, were determined by comparing the instrument response to the calibration curve shown in Fig. 9. This is the same calibration curve used in Task I and was originally to be used only for sample temperatures up to 900 K. During Task I the instrument was calibrated for the elevated temperatures used for Task III except that the carrier gas was argon. Methane modified air was used in Task III and because no calibration curve exists for NO in N_2 at elevated temperatures, the original calibration curve was used and the results compared with the probe values and theoretical results.
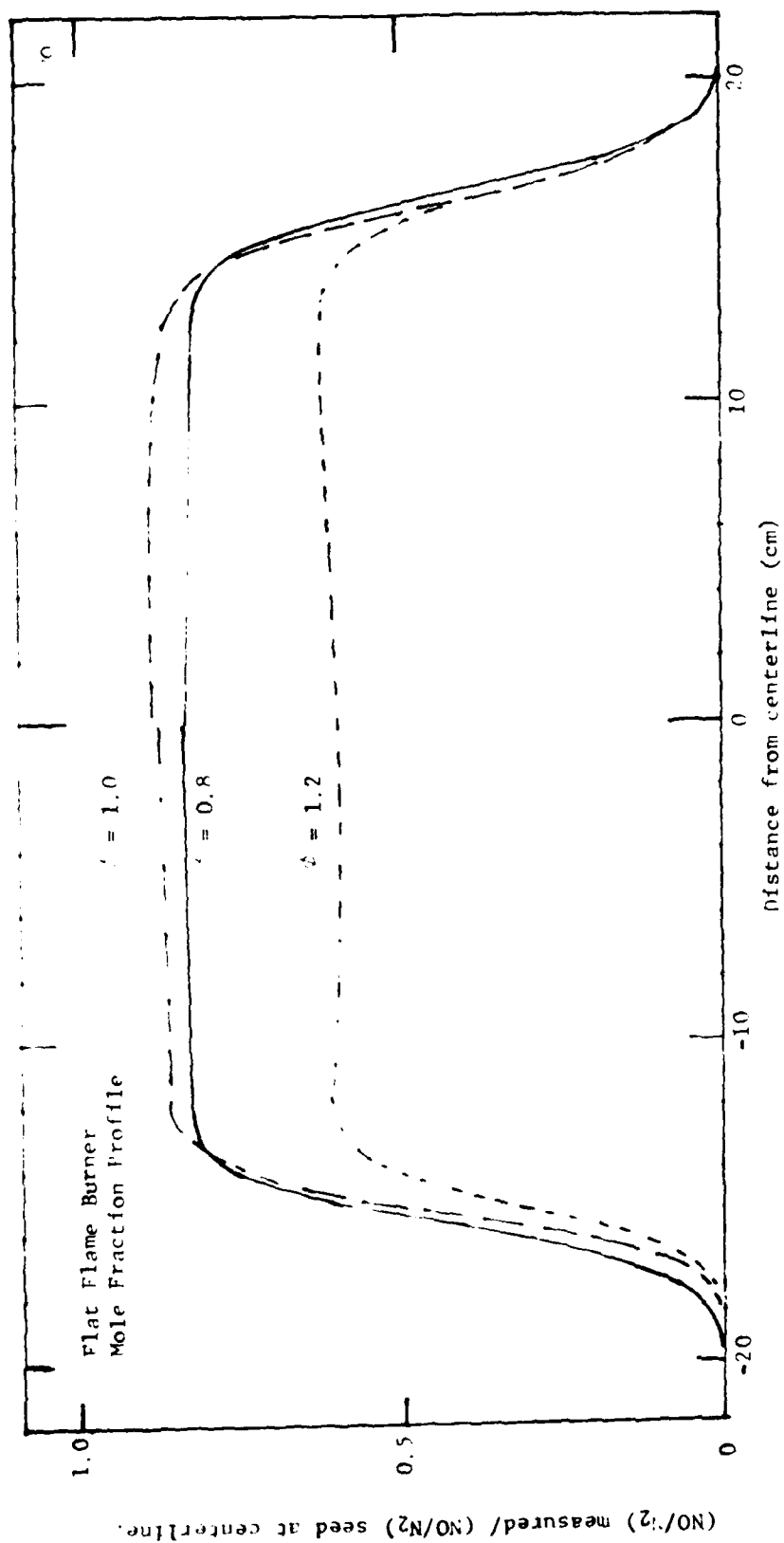
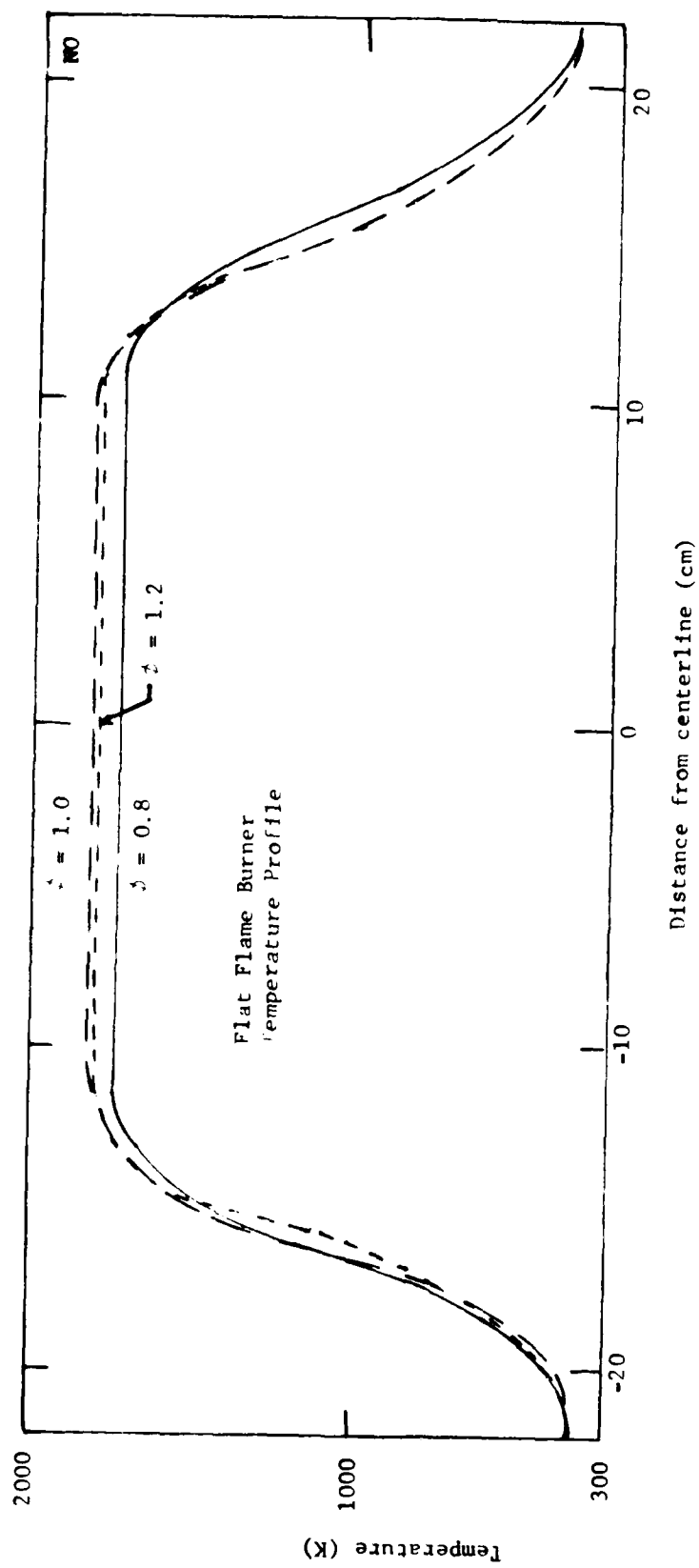**Figure 1.** Mole Fraction Profile for the Flat Flame Burner for three conditions of stoichiometry

Figure 2. Temperature Profile for the Flat Flame Burner for three conditions of stoichiometry
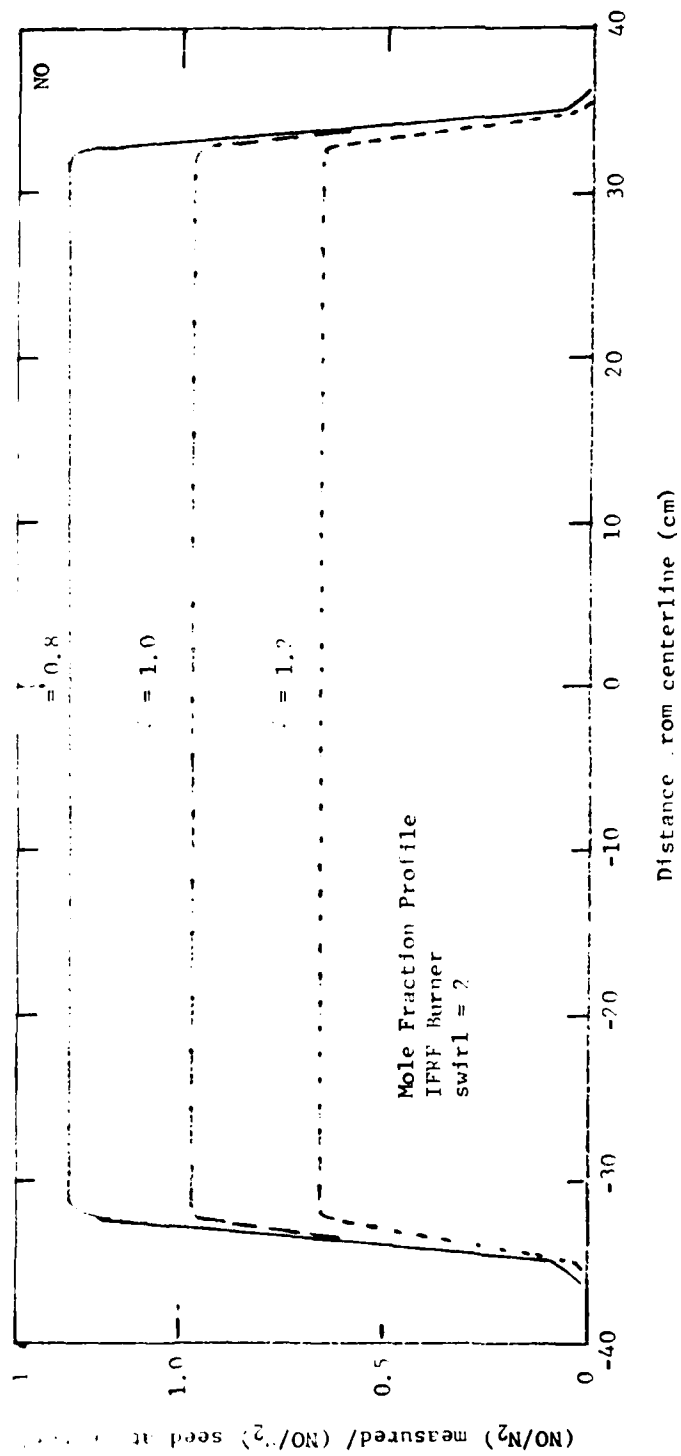
NO

Mole Fraction Profile
IFRF Burner
swirl = 2

= 0.8

= 1.0

= 1.2

(NO/N$_2$) measured/ (NO/N$_2$) seed at ...

Distance from centerline (cm)

Figure 3. Mole Fraction Profile for the IFRF Burner with a swirl of 2 for three conditions of stoichiometry.

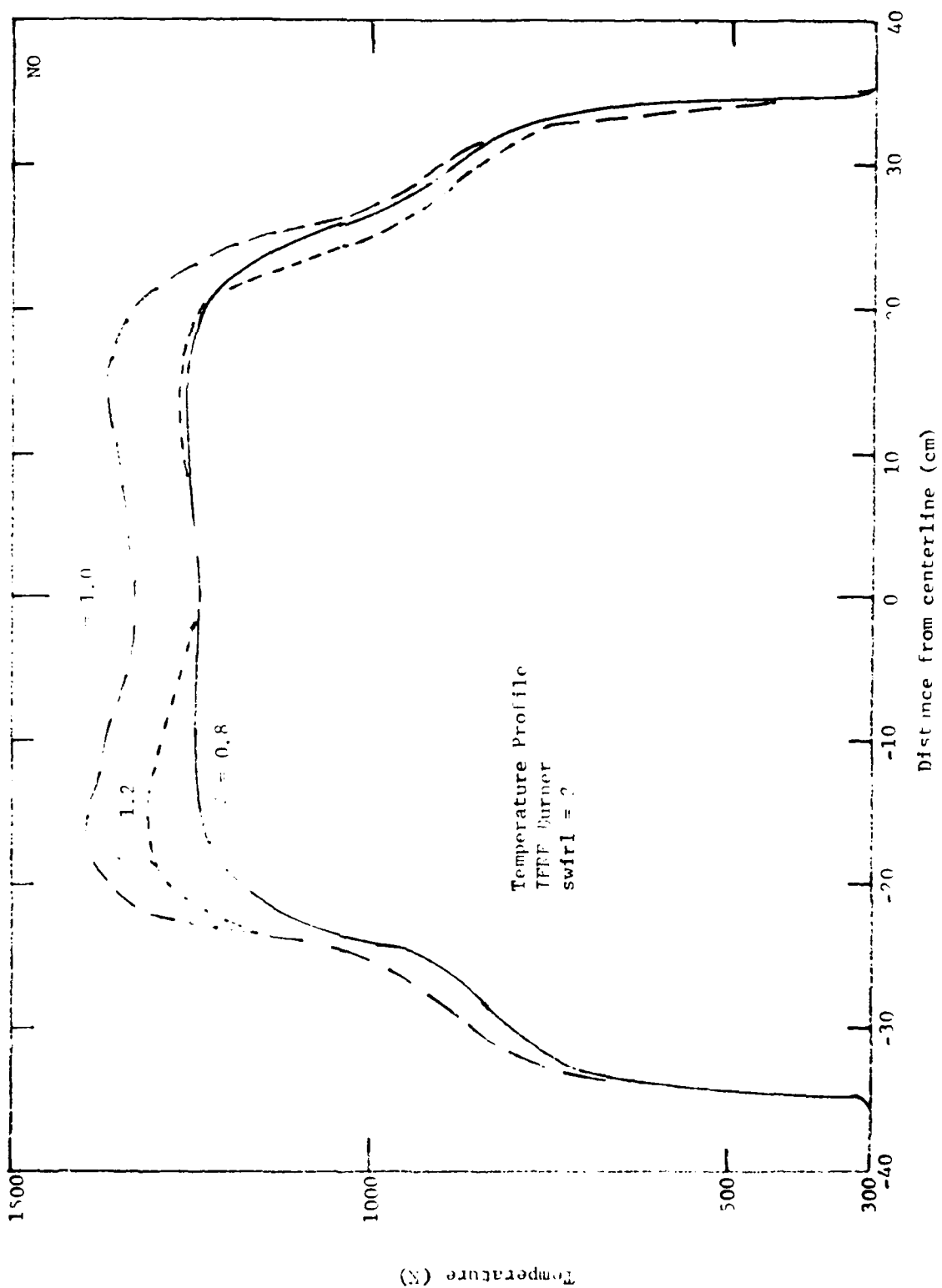Figure 4. Temperature Profile for the IFRF Burner with a swirl of 2 for three conditions of stoichiometry.
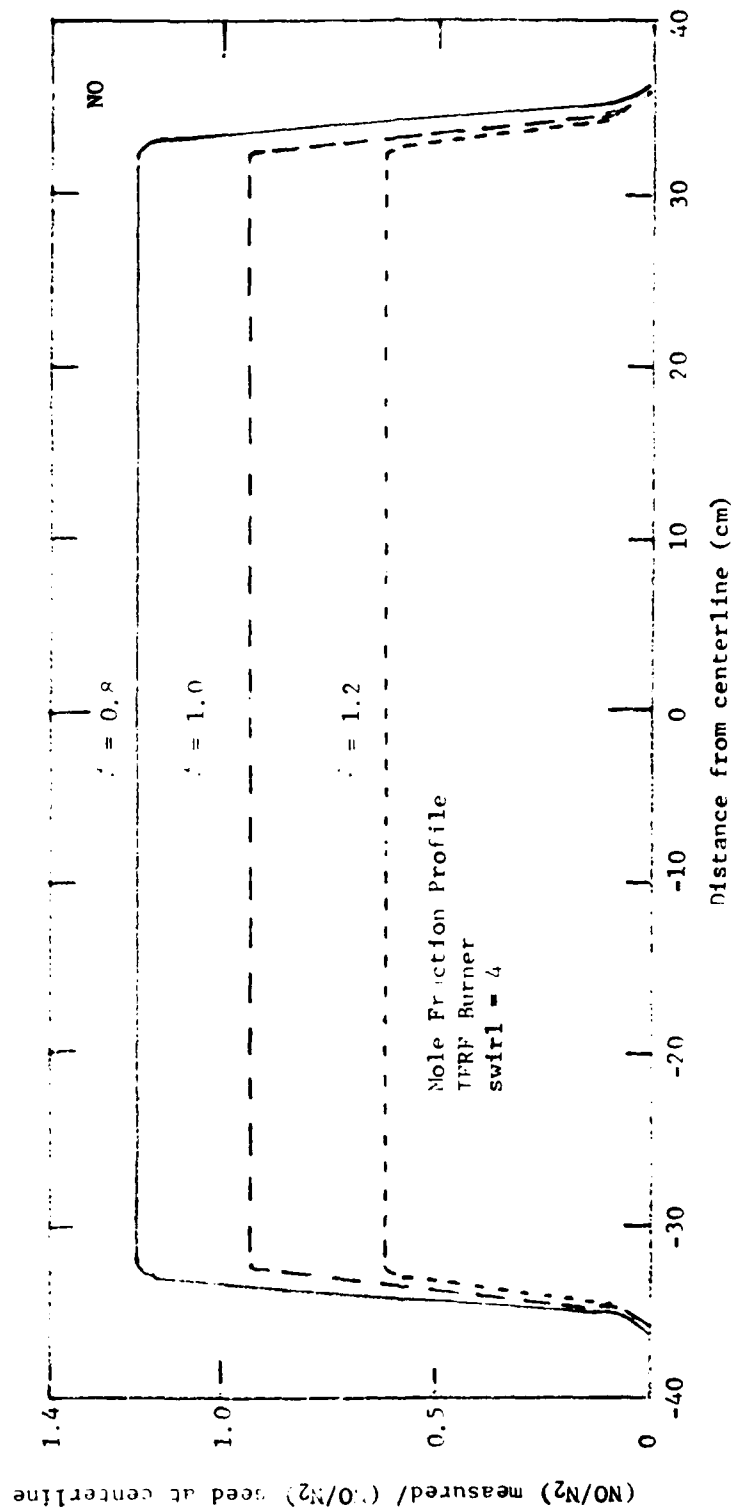
Figure 5. Mole Fraction Profile for the IFRF Burner with a swirl of 4 for three conditions of stoichiometry.
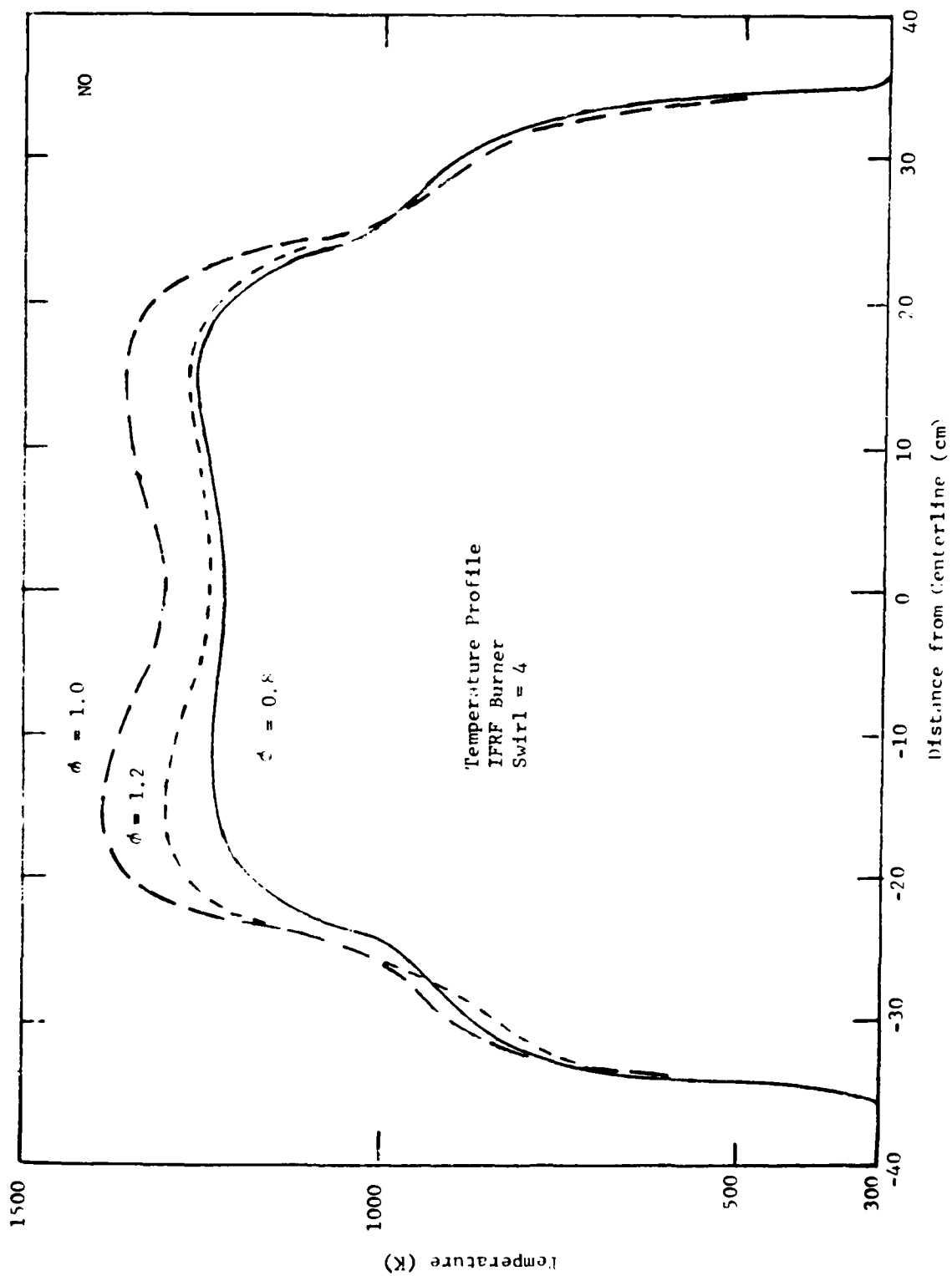
Figure 6. Temperature Profile for the IFRF Burner with a swirl of 4 for three conditions of stoichiometry.
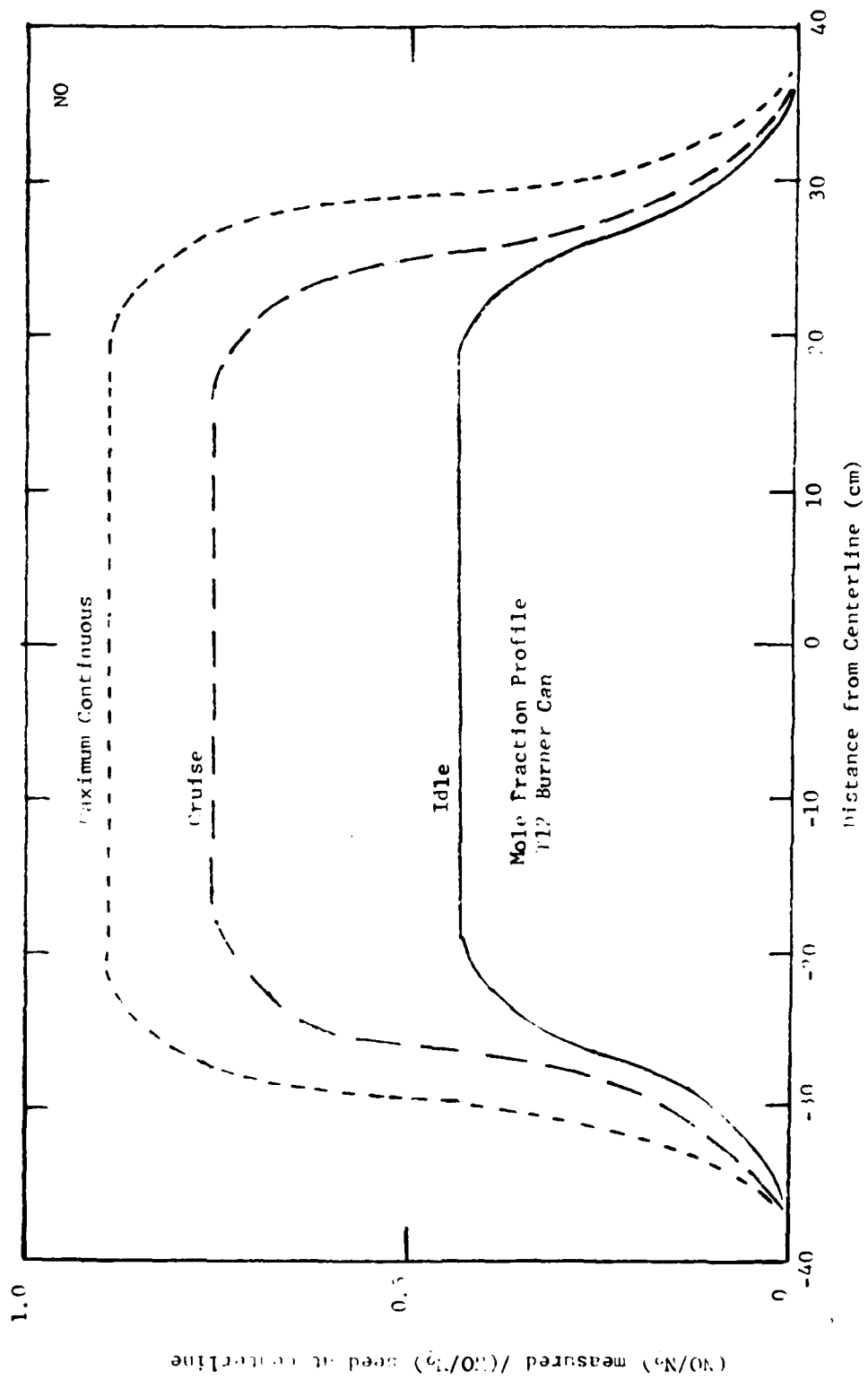
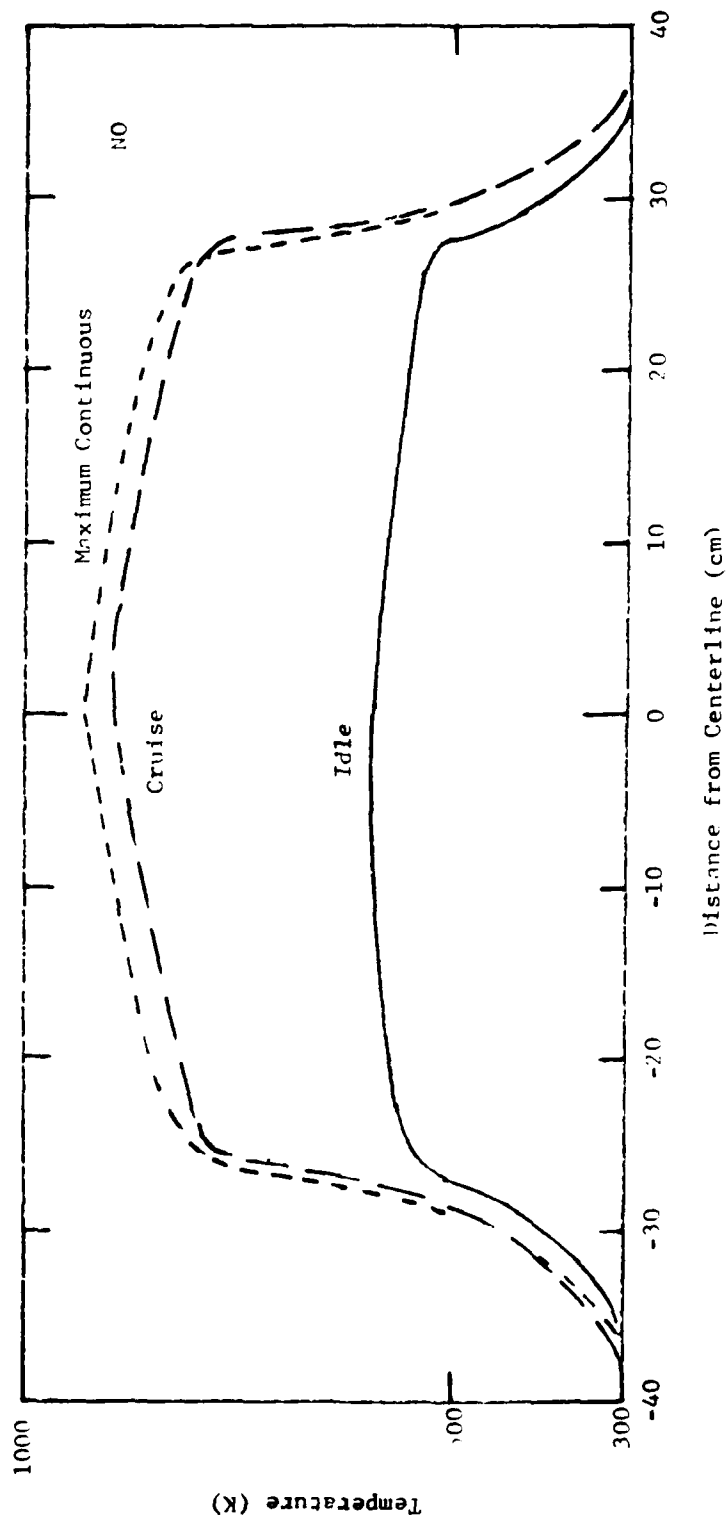Figure 3. Mole Fraction Profile for the FT12 Burner Can for three power conditions.

Figure 8.   Temperature profile for the FT12 Burner Can for three power conditions.
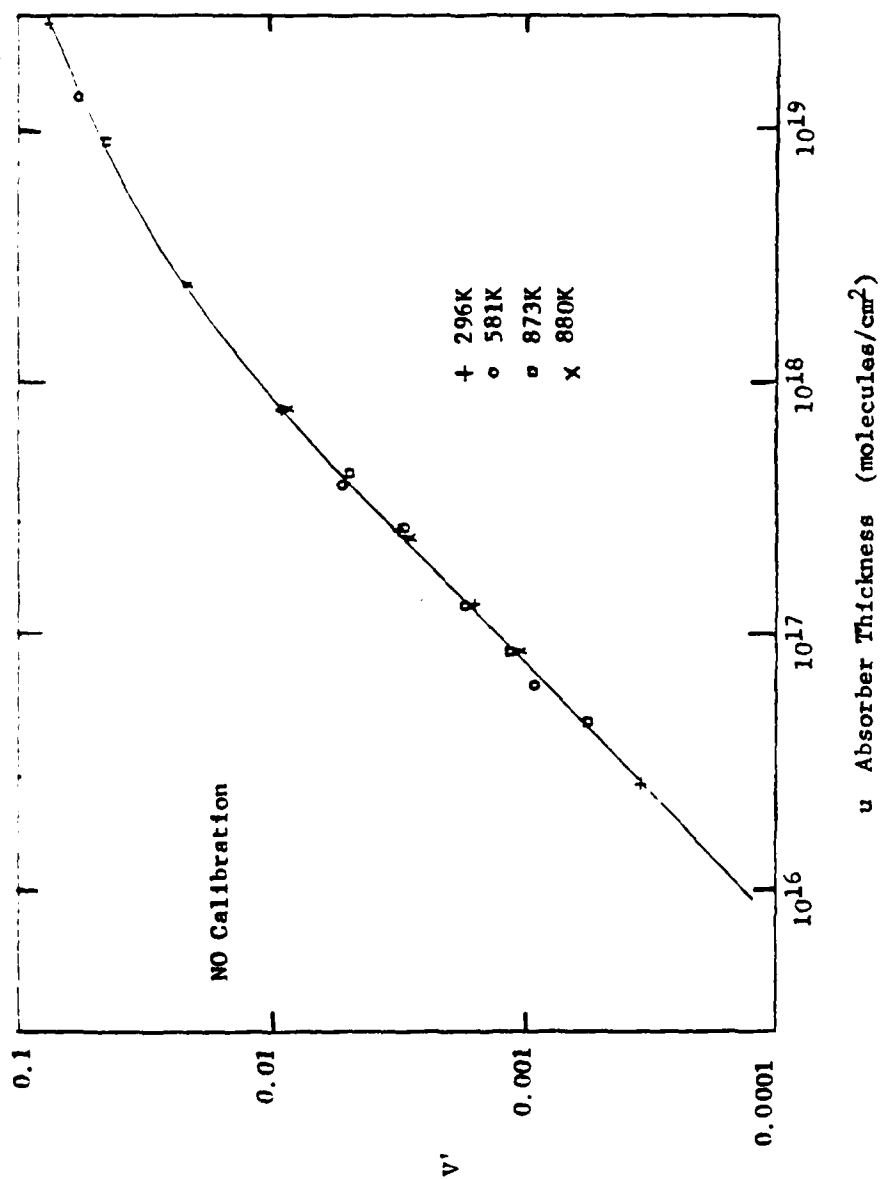
Figure 9. Calibration curve for NO used at Wright Patterson Air Force Base, Instrument response V' vs absorber thickness u.

In order to better understand the effects on the instrument of having the sample at elevated temperatures, calculations were made simulating the instrument response and plotted against the sample temperature. These results are shown as the solid curves in Fig. 10. The values for the 600 K calculations were so close to the 300 K values that a single curve was used for both. The values represented by + were obtained from the original calibration curve and fall on the 300-600 K curve. This indicates the calculations represent the response of the instrument very well for samples at room temperature and supports the validity for the curves for the higher temperature samples. As can be seen in Fig. 10, as the temperature increases the response of the instrument decreases. This temperature dependence was found to be true in Task I and the results of Task III verifies it.

RESULTS

The results of all the tests are tabulated and presented in Tables 1 through 4. The first column lists the test identification number, the second column lists um the absorber thickness of the sample as measured by the smokestack instrument and the third column lists uc, the absorber thickness as calculated from the probe temperature and mole fraction profiles. The fourth column lists the ratio um/uc. The fifth column for the static cell tests, list the temperature of the sample, for the other tests where temperature gradients occur, the centerline temperature of the sample is listed. The stoichiometric conditions were changed for the IFRF and FT12 burner tests and are listed in the sixth column in Tables 2 through 4.

CONCLUSIONS

The values of um/uc are plotted against temperature as dots in Fig. 11. The values represented by the squares were obtained from the curves in Fig. 10. The results are similar to those obtained in Task 1 when argon was used as a carrier gas. The smokestack results tend to be higher, up to 20 percent for temperature below 900 K and tend to be lower, down to 50 percent, for temperatures above 1100 K. The calculated results, represented by the squares, show the same tendency. These calculated values were obtained by determining the ratio of $u(296)/u(\theta)$ for a constant V'. They are within 20 percent of the results determined by the smokestack and probe instruments even at the temperature as high as 1800 to 1900 K. The fact that the ratio, at the two temperatures, of the calculated instrument response closely fits the ratio of the measured to probe results indicates than an instrument using gas correlation techniques, if calibrated for these temperatures could easily predict the amount of NO that was being emitted by a jet engine. Also it verifies that the probe instruments are reasonably accurate even at the higher temperature, certainly not in error by factors of as great as six.
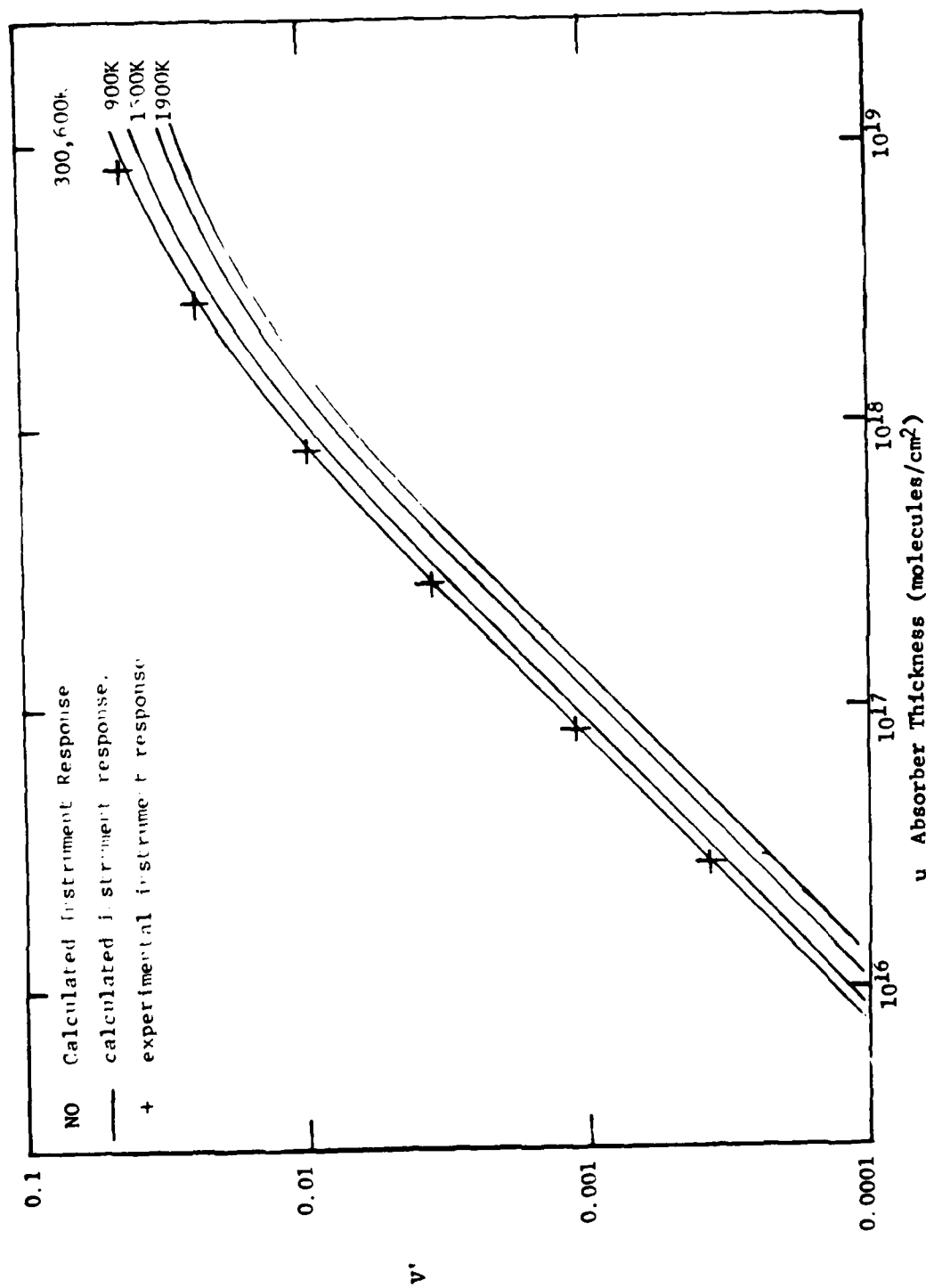
A-12

Figure 10. **Calculated instrument response.** The solid curves represent the calculated instrument response for five different temperatures. The plotted points, +, are values determined from the calibration curve shown in Figure 9.

TABLE 1

STATIC CELL TEST RESULTS

um	uc	um/uc	θ
Multiply values of u by 10^{16} (a) $(\#/cm^2)$	$(\#/cm^2)$		(K)
UTRC TESTS			
52.5	49.5	1.06	296
52.5	49.5	1.06	296
50.5	49.5	1.02	296
50.5	49.5	1.08	296
FORD TEST			
52.5	49.5	1.06	296
49.8	49.5	1.01	296

(a)
The units of u are molecules/cm^2, abbreviated here by $(\#/cm^2)$.

TABLE 2

FT12 BURNER CAN TEST RESULTS

(a) mn	uc	um/uc	θ	(b) Comments
Multiply values of u by 10^{16}			Centerline	
(c) $(\#/cm^2)$	$(\#/cm^2)$		(K)	
FAI-1	45.7	46.5	0.983	590	Idle
FAI-2	53.5	45.5	1.17	590	Idle
FAI-3	34.4	28.5	1.21	590	Idle
FAC-1	29.6	31.2	0.948	900	Cruise
FAC-2	21.3	23.3	0.910	900	Cruise
FAM-1	31.2	39.5	0.789	935	Max
FAM-2	22.9	28.5	0.802	935	Max
FAH-1	54.6	50.2	1.09	500	Air Only

(a) Noise Equivalent u = 1 x 10^{16} molecules/cm^2

(b) Three power conditions were tested, engine at idle, cruise and maximum
     continuous. In addition hot air without the engine running was seeded
     for test FAH-1.

(c) The units of u are molecules/cm^2, abbreviated here by $(\#/cm^2)$

TABLE 3

IFRF BURNER TEST RESULTS

(a) u_m		u_c	u_m/u_c	θ	(b) $_\phi$
Multiply values of u by 10^{16}				Centerline	
(c) $(\#/cm^2)$		$(\#/cm^2)$		(K)	
			Swirl = 0.63		
FA-1-1	11.3	18.5	0.611	1230	0.8
FA-2-1	9.7	12.8	0.756	1330	1.0
FA-3-1	5.3	7.7	0.689	1240	1.2
FA-3-2	6.6	13.7	0.486	1240	1.2
			Swirl = 1.25		
FA-4-1	21.5	34.7	0.620	1220	0.8
FA-5-1	10.0	22.5	0.443	1300	1.0
FA-5-2	14.3	33.8	0.626	1300	1.0
FA-6-1	8.0	13.9	0.578	1235	1.2
FA-6-2	9.7	15.4	0.630	1235	1.2

(a)   Noise Equivalent $u = 1.5 \times 10^{16}$ molecules/cm^2

(b)   Three stoichiometric conditions were tested;
      Lean, ϕ = 0.8, normal, ϕ = 1.0 and rich, ϕ = 1.2

(c)   The units of u are molecules/cm^2, abbreviated here by $(\#/cm^2)$

TABLE 4

FLAT FLAME BURNER TEST RESULTS

(a) um	uc	um/uc	θ	(b) φ
Multiply values of u by 10^{16}			Centerline	
$(\#/cm^2)$	$(\#/cm^2)$		(K)	
FAB1-1 7.4	13.2	0.562	1740	0.8
FAB1-2 11.3	26.9	0.420	1830	0.8
FAB2-1 9.1	23.6	0.388	1830	1.0
FAB301 4.7	7.3	0.641	1800	1.2
FAB3-2 6.9	13.6	0.503	1800	1.2

(a) Noise Equivalent $u = 2 \times 10^{16}$ molecules/cm^2

(b) Three stoichiometric conditions were tested; lean, $\phi = 0.8$, normal, $\phi = 1.0$ and rich, $\phi = 1.2$

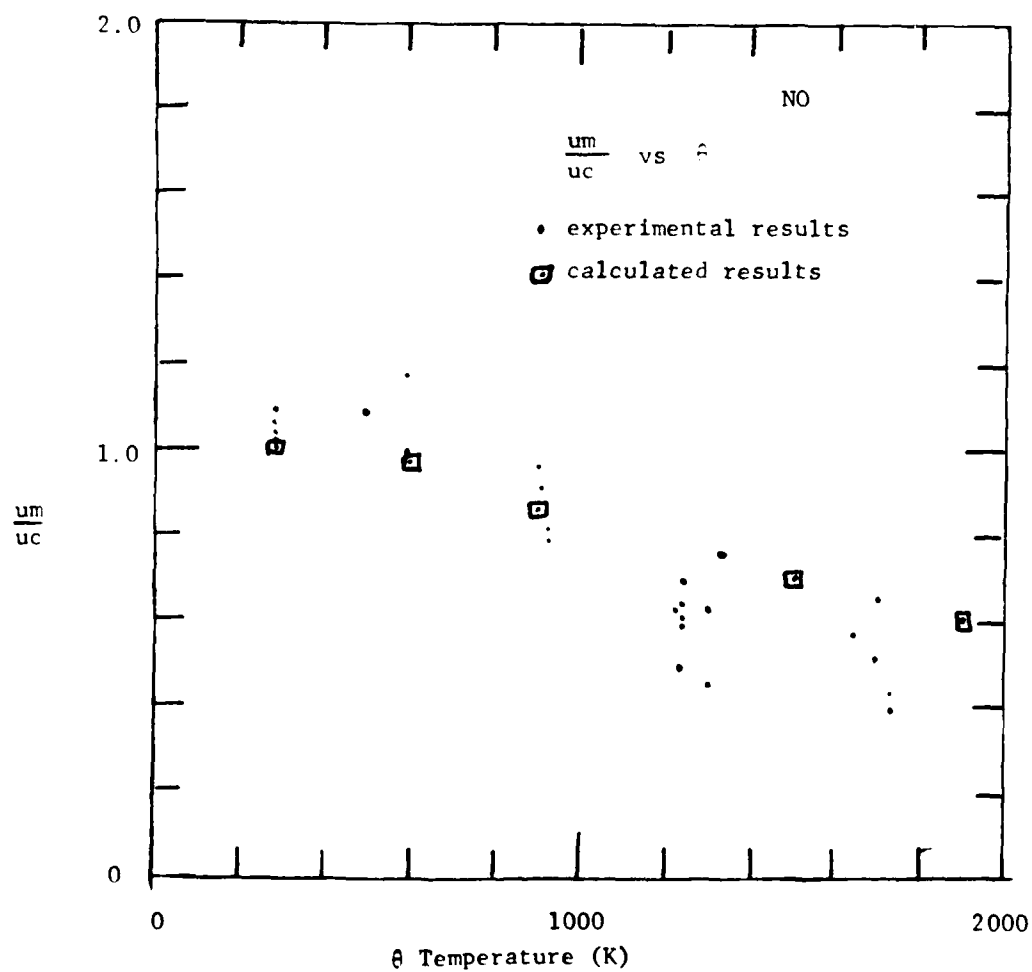(c) The units of u are molecules/cm, abbreviated here by ($\#/cm^2$)

Figure 11. Plot of um/uc versus temperature. The points are from the results tabulated in tables 1 thru 4. The values represented by the squares, ▣ , are from the calculated ratio u(296)/u(θ) for a constant V'.

REFERENCES

1. Burch E. E. and Gryvnak D. A.: "Infrared Gas Filter Correlation
   Instrument for In Situ Measurement of Gaseous Pollutants" prepared
   by Ford Aerospace and Communications Corp. for the EPA under Contract
   No. 68-02-0575, EPA Report No. 65012-24-094, December 1974.

END

DATE
FILMED

5 81

DTIC